AD-A061 880 GENERAL ELECTRIC CORPORATE RESEARCH AND DEVELOPMENT --ETC F/G 11/2
DEVELOPMENT OF A SINTERING PROCESS FOR HIGH-PERFORMANCE SILICON--ETC(U)
JUL 78 S PROCHAZKA, C D GRESKOVICH DAAG46-77-C-0030

UNCLASSIFIED SRD-77-178 AMMRC-TR-78-32 NL

1 OF 2
ADA
061880

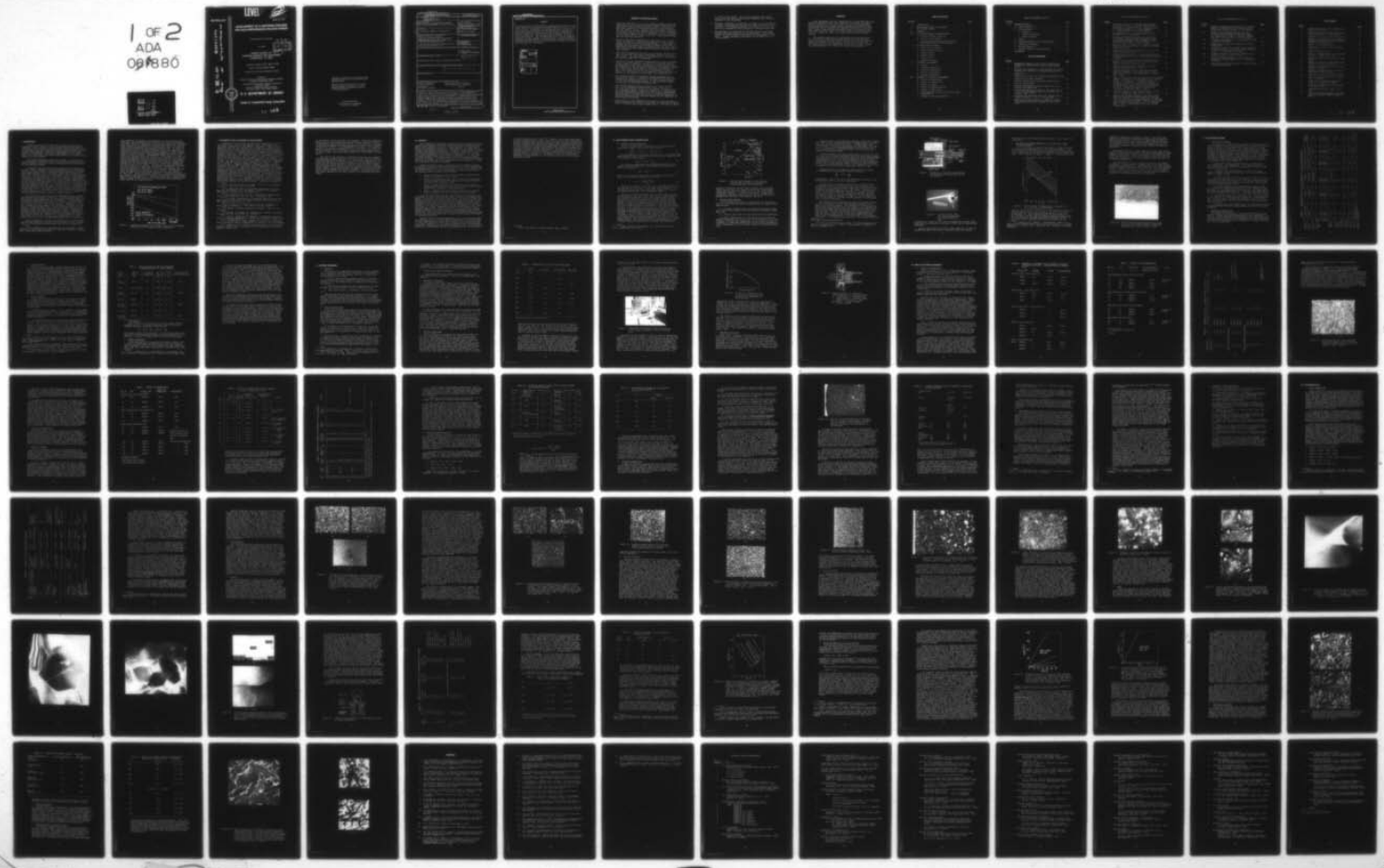

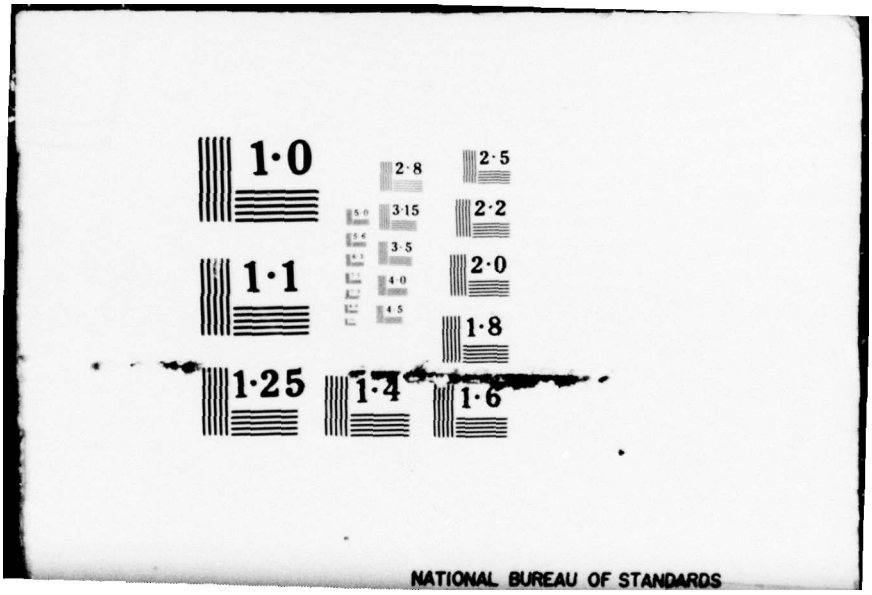
1·0
1·1
1·25
1·4
1·6
1·8
2·0
2·2
2·5
2·8
3·15
3·5
4·0
4·5
5·0
5·6
NATIONAL BUREAU OF STANDARDS

AMMRC TR 78-32

DEVELOPMENT OF A SINTERING PROCESS FOR HIGH-PERFORMANCE SILICON NITRIDE

S. Prochazka and C. D. Greskovich

July 1978

GENERAL ELECTRIC CO.
CORPORATE RESEARCH AND DEVELOPMENT
SCHENECTADY, NY 12301

Final Report - March 15, 1977 - March 15, 1978

Contract Number DAAG46-77-C-0030

Prepared for
ARMY MATERIALS AND MECHANICS RESEARCH CENTER
Watertown, Massachusetts 02172

under AMMRC/DOE Interagency Agreement EC-76-A-1017
Department of Energy
Division of Transportation Energy Conservation
Heat Engine Highway Vehicle Systems Program

U. S. DEPARTMENT OF ENERGY

Division of Transportation Energy Conservation

The findings in this report are not to be construed as an official Department of the Army position, unless so designated by other authorized documents.

Mention of any trade names or manufacturers in this report shall not be construed as advertising nor as an official indorsement or approval of such products or companies by the United States Government.

DISPOSITION INSTRUCTIONS

Destroy this report when it is no longer needed.
Do not return it to the originator.

UNCLASSIFIED

SECURITY CLASSIFICATION OF THIS PAGE (When Data Entered)

REPORT DOCUMENTATION PAGE

READ INSTRUCTIONS BEFORE COMPLETING FORM

1. REPORT NUMBER: AMMRC TR-78-32	2. GOVT ACCESSION NO.
3. RECIPIENT'S CATALOG NUMBER	
4. TITLE (and Subtitle): DEVELOPMENT OF A SINTERING PROCESS FOR HIGH-PERFORMANCE SILICON NITRIDE	5. TYPE OF REPORT & PERIOD COVERED: Final Report - March 15, 1977-March 15, 1978
6. PERFORMING ORG. REPORT NUMBER: SRD-77-178	
7. AUTHOR(s): S. Prochazka and C.D. Greskovich	8. CONTRACT OR GRANT NUMBER(s): DAAG46-77-C-0030
9. PERFORMING ORGANIZATION NAME AND ADDRESS: General Electric Company, Corporate Research and Development, Schenectady, New York 12301	10. PROGRAM ELEMENT, PROJECT, TASK AREA & WORK UNIT NUMBERS
11. CONTROLLING OFFICE NAME AND ADDRESS: Army Materials and Mechanics Research Center, Watertown, Massachusetts 02172	12. REPORT DATE: July 1978 13. NUMBER OF PAGES: 77
14. MONITORING AGENCY NAME & ADDRESS (if different from Controlling Office)	15. SECURITY CLASS. (of this report): Unclassified 15a. DECLASSIFICATION/DOWNGRADING SCHEDULE

16. DISTRIBUTION STATEMENT (of this Report)

Approved for public release; distribution unlimited.

12 97 p.

17. DISTRIBUTION STATEMENT (of the abstract entered in Block 20, if different from Report)

9 Final rept. 15 Mar 77-15 Mar 78,

18. SUPPLEMENTARY NOTES

19. KEY WORDS (Continue on reverse side if necessary and identify by block number)

Ceramic Materials
Silicon Nitride
Sintering
Nitrogen Ceramics
Beryllium Silicon Nitride
High Temperature Properties
→ Beta

20. ABSTRACT (Continue on reverse side if necessary and identify by block number)

β-Si_3N_4 ceramics with excellent creep and oxidation resistance in the temperature range of 1300 to 1450°C can be produced by the sintering process using small amounts (3-7%) of $BeSiN_2$ as a densification aid. These ceramics are composed of both elongated and equi-axed grains of *β-Si_3N_4 solid solution and sometimes contain minor amounts of Si, SiC and $BeSiN_2$, depending on starting composition and sintering conditions. Although samples have been occasionally

DD FORM 1 JAN 73 1473 EDITION OF 1 NOV 65 IS OBSOLETE

UNCLASSIFIED

SECURITY CLASSIFICATION OF THIS PAGE (When Data Entered)

* Beta

406 627

Block No. 20

ABSTRACT

sintered to 98% relative density, densities near 90% are routinely produced by sintering at 2000-2100°C for 15 min. in 60-80 atm of N_2. In addition to optimum amounts of Be and O required for the attainment of high density and consequently, good thermochemical properties of the ceramic, effects of metallic impurities (Ca, Mg and Fe which promote sintering) have been observed. The thermodynamic stability of Si_3N_4 is outlined and the "region of sinterability" is established for submicron α-Si_3N_4 powders containing small amounts of $BeSiN_2$. Proposed chemical reactions and mechanism of densification during sintering are discussed.

alpha

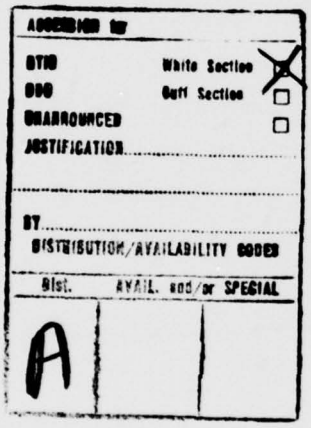

SUMMARY OF IMPORTANT RESULTS

1. Beryllium additions (0.5 to 1.0%) added as $BeSiN_2$ induce densification in silicon nitride powder compacts when heated to 2000-2100°C under 4-8 MPa nitrogen pressure. Sintering to densities above 90% is obtained only with powders which contain at least 2% oxygen. Powders with less oxygen respond if the oxygen level is increased by addition of SiO_2 or exposure of the green compacts to air at 850-900°C prior to sintering. Loss of oxygen during sintering results in nonuniform shrinkage and low final densities.

2. Metallic impurities, especially Ca, Mg, Fe on a 0.1 to 0.2% level, and typical for high grade commercial Si_3N_4 powders, promote sintering of beryllium-added powders. Five different powders were processed and sintered to densities near 90%. High density material could be produced from very pure powders under conditions which made possible impurity transport during sintering.

3. The sintering operation was done in an envelope of dense SiC, tube or crucible form with the specimens usually covered by pack powder. The pack powder is not essential to the sintering process under such circumstances.

4. Sintering of Si_3N_4 requires ultimate particle size corresponding to a specific surface area 10-15 m^2/g and good particle packing during compaction. Crystalline silicon nitrides may be comminuted to the required fineness by extended ball milling with steel balls and by removing iron wear by leaching with HCl. The oxygen pick-up due to this processing is small, about 0.07% oxygen per m^2 of new specific surface area and not harmful to the composition when taken into consideration.

5. The nitrogen pressure required to prevent decomposition on sintering of Si_3N_4 is in approximate agreement with data calculated from chemical equilibria. Nitrogen pressures about 4 times the decomposition pressure at the sintering temperature results in successful sintering runs.

6. The sintered bodies consist of grains of a solid solution near the stoichiometric composition of $Si_{2.9}\ Be_{0.1}\ N_{3.8}\ O_{0.2}$ and minor amounts of SiC, Si and $BeSiN_2$. A small amount of an amorphous phase is sometimes detectable by transmission electron microscopy particularly in the lattice imaging mode. The occurrence of the minority phases is strongly dependent on starting composition and sintering conditions and sometimes is nonuniformly distributed.

7. Creep testing of two compositions carried out in three point bending shows strain rates not measurable at 1300°C and 69 MN/m^2 i.e. $> 3 \times 10^{-6}$/h outer fiber strain, and 3×10^{-4} and 2×10^{-5}/h

at 1450°C and 69 MN/m^2. These values approach the lowest creep rates for any silicon nitride (excluding CVD) material reported in the literature.

8. Oxidation resistance is excellent at 1400°C in air and depends strongly on residual porosity and the level of metallic impurities. The oxidation product is cristobalite in pure materials and cristobalite plus phenacite in less pure materials.

9. Microhardness is controlled by residual porosity and ranges between 1400-1800 kg/mm^2 for 95 to 99% density. The elastic modulus is between 269 and 276 GN/m^2 and also depends on porosity. Thermal expansion coefficient for 25-1000°C is 3.37 - 3.54 x 10^{-6}/°C.

FOREWORD

This development has been sponsored by the Army Materials and Mechanics Research Center under AMMRC/DOE Interagency Agreement EC-76-A-1017-002 as part of the DOE, Division of Transportation Energy Conservation, Highway Vehicle Systems Heat Engine Program and carried out in the Physical Chemistry Laboratory of the General Electric Research and Development Center, Schenectady, New York, under Contract DAAG46-77-C-0300 during the period of March 15, 1977 - March 15, 1978. Mr. George Gazza was the Program monitor.

The authors would like to acknowledge the contribution of Dr. Victor Lou of Case Western Reserve University for the TEM study of some materials by lattice imaging, and also the TEM work done by I.L. Mella. The processing skills of C. O'Clair and C.F. Bobik were of great assistance in the present work. Thanks are also extended to L. D'Amico for manuscript preparation.

TABLE OF CONTENTS

TABLE OF CONTENTS (Cont'd)

LIST OF ILLUSTRATIONS

LIST OF ILLUSTRATIONS (Cont'd)

LIST OF ILLUSTRATIONS (cont'd)

LIST OF TABLES

I. INTRODUCTION

Ceramics have been considered as structural materials for components of heat engines. Such applications require complex components with accurate tolerances which in many instances cannot be machined or are prohibitively expensive when machined from hot-pressed stock material. Therefore, developments of processes which use conventional fabrication techniques for new ceramics, such as SiC and Si_3N_4, can lead to mass production of ceramic components for heat engines.

This program addresses sintering of Si_3N_4. Its objectives are to develop a sinterable form of Si_3N_4 with improved high temperature behavior and to evaluate microstructures and properties of the resulting ceramic.

A study of Si_3N_4 sintering was initiated in this laboratory in 1976, within a broader program investigating the sintering behavior of covalent solids. The program was supported by an ARPA grant under contract F33615-76-C-5033, which was terminated in July 1976, and the results were discussed in final report AFML-TR-76-179.[1] It was shown that a very fine, very pure Si_3N_4 powder, synthesized from SiH_4 and NH_3, could be sintered to high density if additions of Mg_3N_2 and Be_3N_2 were used to promote densification and if the sintering was carried out under 5-8 MPa (50-80 atm.) nitrogen pressure at 1800-2000°C. Both amorphous and crystalline forms of Si_3N_4 responded favorably under these conditions, but amorphous starting materials would in some instances result in disruption of the specimens due to the spontaneous amorphous-to-crystalline transition near 1500°C. Specimens sintered near 1900°C were composed of fine equiaxed grains of β-Si_3N_4, those sintered at 2000° or above showed strong anisotropic growth of prismatic grains.

The present work made possible by AMMRC/DOE support extends the materials development initiated in the AFML program mentioned above and strongly emphasizes the development of understanding of the physical mechanisms involved in sintering. In the following we report on work done during March 15, 1977 to March 14, 1978, i.e., during the first year of this program. Sintering of a number of starting Si_3N_4, powders with additions of $BeSiN_2$ has been achieved. Sintered densities in the low nineties have been obtained routinely; however, high densities, close to theoretical, although occasionally observed, have been elusive. According to available X-ray and analytical evidence, the sintered bodies in the selected system are composed of a solid solution of a composition close to $Si_{2.9}\ Be_{0.1}\ N_{3.8}\ O_{0.2}$ and less than 2% of other phases such as Si, SiC, and additional phases not yet identified.

The development of a process for fabrication of a sinterable single phase high grade silicon nitride ceramic has been a difficult task compounded by effects which were not anticipated and

---

[1] C.D. Greskovich, S. Prochazka and J.H. Rosolowski, "Basic Research on Technology Development for Sintered Ceramics," November 1976, Final Report AFML-TR-76-179.

only gradually recognized. Nevertheless, decisive progress has been made, and the mechanisms of sintering in silicon nitride compositions containing beryllium are now better understood. Measurements carried out on laboratory specimens show that a silicon nitride ceramic surpassing all known hot-pressed forms in creep and oxidation resistance has been synthesized thus far. One of our future goals will be to prepare sintered Si_3N_4 with improved high temperature stress rupture performance comparable to that recently found for General Electric's hot pressed Si_3N_4 containing 7 wt% $BeSiN_2$ in solid solution. See Figure 1. This figure is a plot of normalized strength retention versus time to failure in an air (oxidizing) atmosphere for GE hot pressed Si_3N_4 and the best commercially-available hot-pressed Si_3N_4, Norton's NC-132. These plots demonstrate that the strength retention of GE HPSN at 1400°C far exceeds that of Norton's NC-132 Si_3N_4 at 1400°C and even exceeds the Norton material at 1200°C. For example, although NC-132 Si_3N_4 has a very high room temperature strength of 125,000 psi, the strength retention is only about 35% of the room temperature value after an exposure of 2 minutes in air at 1400°C. In contrast, under the same conditions GE HPSN exhibits a strength retention of about 90%. These outstanding properties of beryllium-containing hot pressed Si_3N_4 provide the stimulus to establish a technological base for the development of a sintering process which enables large, complex shapes of high density to be fabricated with much lower costs than the hot pressing route.

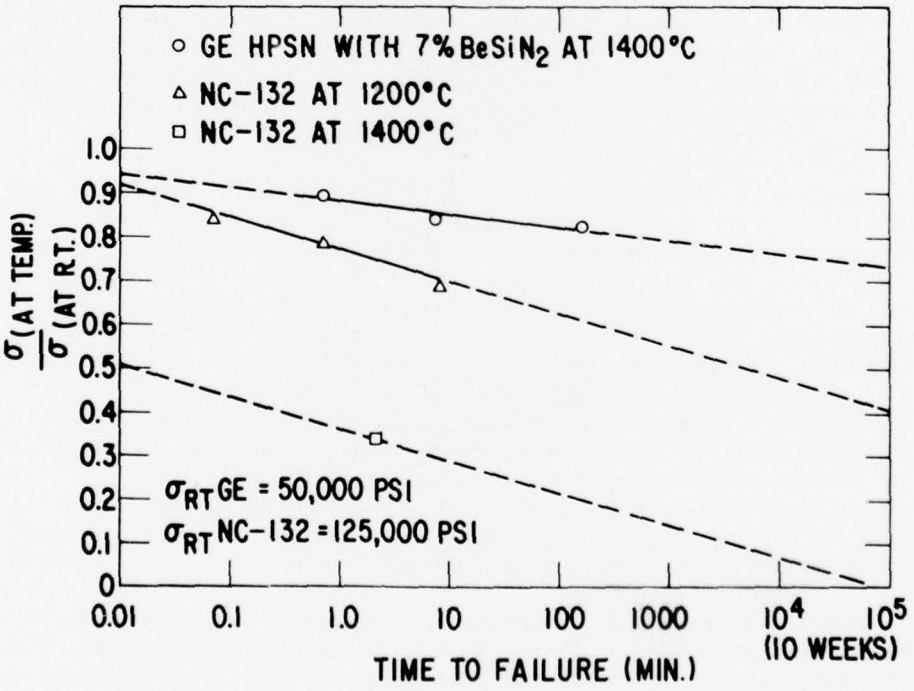

Figure 1. Normalized strength versus time-to-failure for GE-HPSN and Norton NC-132 Si_3N_4 at high temperatures.

II. THE PRESENT STATUS OF SINTERING OF SILICON NITRIDE

Sintering in silicon nitride was first reported by Terwilliger and Lange[2] who demonstrated densification in specimens of a Si_3N_4-MgO composition at 1550-1650°C in nitrogen. They achieved densities near 90% and observed that thermal dissociation interfered with the sintering process and limited the attainable degree of densification. At present this task is studied by a number of research groups with emphasizing different metal oxides as sintering promoting additions. D.J. Rowcliffe and P.J. Jorgensen[3] of S.R.I. and Buljan and Kleiner[4] and J.T. Smith of GTE[5] developed sintering in the Si_3N_4-Y_2O_3 oxide systems to nearly full density. H.F. Priest, G.L. Priest and G.E. Gazza of AMMRC have studied additions of CeO_2, MgO and Y_2O_3,[6] and M. Mitomo[7], M. Tsutsumi, E. Bannai and T. Tanaka[8] sintered Si_3N_4 with addition of MgO. I. Oda, M. Kaneno and N. Yamamoto studied the system Si_3N_4-MgO-BeO and Si_3N_4-MgO-BeO-CeO_2.[9] Additional work in the system Si_3N_4-Al_2O_3-ZrO_2 is in progress at Max Planck Institute[10] and in the system Si_3N_4-Al_2O_3-Y_2O_3 in a program of Toyota-Tokyo Shibaura El. Co.[11] Substantial progress has been made in processing, and fabrication of complex components has been demonstrated. Information on basic thermomechanical properties of the new materials is gradually becoming available and shows, as expected, similar trends as in hot-pressed materials. It is reasonable to expect, that with further advancement, material with properties nearly equivalent to present hot-pressed compositions may be obtained. Only scant information

---

(2) G.R. Terwilliger and F.F. Lange, "Pressureless Sintering of Si_3N_4" J. Mat. Sci., 10, 1169(1975).

(3) D.J. Rowcliffe and P.J. Jorgensen "Sintering of Silicon Nitride," Proceedings of the Workshop in Ceramics for Advanced Heat Engines, January 1977, F.C. Moore, ed.

(4) S.T. Buljan and R.N. Kleiner, "Cold Pressed and Sintered Si_3N_4" Annual Meeting of Am. Cer. Soc., Cincinnati, 1976.

(5) J.T. Smith, "Properties of Fully Dense Sintered Si_3N_4 Composition," Fall Meeting of the Basic Science Group of the Am. Cer. Soc., Hyannis, Massachusetts, 1977.

(6) H.F. Priest, G.L. Priest and G.E. Gazza, "Sintering of Si_3N_4 under N_2 Pressure," J. Am. Ceram. Soc., 60, 81(1977)

(7) M. Mitomo, "Pressure Sintering of Si_3N_4" J. Mat. Sci. 11, 1103(1976).

(8) M. Mitomo, M. Tsutsumi, E. Bannai and T. Tanaka, "Sintering of Si_3N_4" Am. Cer. Soc. Bull. 55, 313(1976).

(9) I. Oda, M. Kaneno and N. Yamamoto, "Pressureless Sintered Si_3N_4" in Nitrogen Ceramics, F.L. Riley, ed., Noordhoff Layden, 1977

(10) N. Clausen and J. Jahn, "Mechanical Properties of Sintered and Hot Pressed Si_3N_4-ZrO_2 Composites," J. Am. Cer. Soc. 61, 94(1978).

(11) K. Komeya, et al., "Silicon Nitride Ceramics for Gas Turbine Engines," Paper No. 65, Proceeding of the Tokyo Joint Gas Turbine Congress, Tokyo, 1977.

on the details of the processes is available. Generally commercial medium purity grade Si_3N_4 starting powders have been used, milled in nonaqueous dispersions with alumina, silicon nitride or cemented carbide balls, shaped to obtain maximum green density and sintered at 1750° to 1950°C at 2-20 atmospheres of nitrogen. The resulting ceramics are generally composed of very fine grains of β-Si_3N_4 or β solid solutions ($\approx 1\mu$) and variable amounts of other phases, up to 30 vol% of metal oxynitrides and oxides, both crystalline and amorphous.

The role of the additions in sintering of Si_3N_4 is to enhance internal mass transport which occurs, most likely, by the dissolution-reprecipitation mechanism. It is generally accepted that the liquids providing the transport path have to have substantial solubility for the solid and zero or close to zero interfacial angle. The extraneous phases generated from the liquid phase on solidification control all structure sensitive properties, such as strength, creep, stress rupture and fracture toughness in ways which are not predictable by present theoretical concepts. From this point of view every composition is unique and has to be characterized separately.

III. APPROACH

High temperature mechanical properties such as creep and stress rupture are probably controlled by the same atomic mobility as the densification process by which a ceramic material is consolidated during hot-pressing or sintering. Consequently, the higher the necessary consolidation temperature, the better is the chance to obtain a stable high temperature material. Contrary, therefore, to the usual trend dominating current ceramic fabrication, i.e., to lower the process temperature, one strives to increase it. In the case of Si_3N_4, however, difficulties arise due to the limited thermal stability of Si_3N_4. In other words, one has to accept the inconvenience of processing under high temperature and gas pressure, a practice heretofore unusual in ceramics.

Another problem is that, according to all available evidence, Si_3N_4 does not densify without the presence of a liquid phase which in instances solidifies, at least partly, as glass. To minimize the detrimental effect of such a second phase on the refactoriness of the product several options are available:

a. select a composition with a high solidus temperature and minimize the volume of the liquid

b. select the composition such that on cooling, crystallization of a stable refractory phase occurs which eliminates or reduces the volume of liquid

c. select a composition where the additives which promote sintering may ultimately dissolve in Si_3N_4 to form a single phase system (transient liquid sintering)

d. select a composition which enables elimination of second phase by vaporization during extended heat treatment.

Prior work has shown that the liquid phases which promote densification in current hot-pressed forms of Si_3N_4 are primarily composed of silicates and silicon oxynitrides. In order to reduce the amount of silicates or possibly even avoid them, we decided to apply additions in the form of nitrides and to compensate for the lost sinterability by increasing the sintering temperature and nitrogen pressure. The endeavor to prepare a material without a grain boundary phase is, in part, substantiated by the belief that an intergranular oxide phase, typical for current Si_3N_4 ceramics, promotes oxygen transport along grain boundaries particularly under stress conditions. Such a process involving stress enhanced diffusion then results in poor creep resistance and poor stress rupture performance in polyphase materials.

Silicon nitride can be consolidated only with sintering promoting additions and, if a single phase composition is to result, the selected addition has to react with Si_3N_4 to form a solid solution. A convenient addition of this type is alumina or more specifically $Al_2O_3 \cdot AlN$. Materials in the system Si_3N_4-SiO_2-Al_2O_3 - AlN have been extensively investigated by many investigators since the discovery

of solid solubility by K. Jack.[12] However, the results have been at great variance and in general have not, thus far, met expectations. Another substance known to have high solubility in Si_3N_4 is beryllium. An early investigation showed that Be_3N_2 indeed promoted sintering of Si_3N_4 particularly if combined with additions of Mg_3N_2 and the sintering was carried out between 1800-2000°C under sufficient pressure of nitrogen to prevent thermal dissociation. Preliminary oxidation tests revealed, however, that the presence of magnesium at a level of 1% was detrimental to oxidation resistance and that hot-pressed Mg-free compositions were superior to any material from the Si_3N_4 family. Therefore, the development of a sinterable material in the Si_3N_4-Be system was chosen.

---

[12] K.H. Jack and W.J. Wilson, Nature, 283, 28(1972).

IV. SOME THERMODYNAMIC CONSIDERATIONS

A. Silicon Nitride Stability

Silicon nitride powder decomposes at high temperatures, above about 1500°C, into silicon and nitrogen:

$$Si_3N_4 = 3Si_{(l)} + 2N_{2(g)};\ \Delta G_f \qquad (1)$$

If the ambient silicon vapor pressure, P_{Si}, is less than the vapor pressure above liquid silicon, silicon will evaporate and no condensed silicon appears:

$$Si_{(l)} = Si_{(v)};\ \Delta G_{(v)} \qquad (2)$$

At a certain temperature the nitrogen pressure and the silicon vapor pressure are in equilibrium with Si_3N_4 and are related by equation (3).

$$P_{Si}{}^3 \times P_{N_2}{}^2 = K \qquad (3)$$

where K, the equilibrium constant, is related to the sum of the free energies of reactions (1) and (2):

$$K = e - \frac{\Delta G_{(f)} + 3\Delta G_{(v)}}{RT} \qquad (4)$$

The partial pressure of silicon at a selected temperature and nitrogen pressure can be calculated from equation (3). Using data for $\Delta G_{(f)}$ and $\Delta G_{(v)}$ from JANAF Tables,[13] P_{Si} were calculated and plotted in the diagram on Figure 2.

The set of lines from lower right to upper left are isotherms and the solid curve from lower left to upper right is the condensed Si-silicon nitride - gas coexistence boundary and depicts nitrogen pressures above which silicon nitride exists as a solid if silicon vapor is not removed from the system. It has to be emphasized that even at high nitrogen pressure Si_3N_4 will tend to decompose if silicon vapor transport out of the system is not prevented. The role of nitrogen pressure is to decrease P_{Si} such that it is below the vapor pressure in equilibrium with liquid silicon and to prevent spontaneous decomposition of Si_3N_4 into liquid silicon and nitrogen. If, for example, Si_3N_4 is kept at 2000°C in an environment of P_{N_2} at 5 atm it will evaporate, and the rate of evaporation will be controlled either by the rate of silicon vapor transport away from the specimen or by the rate of Si_3N_4 decomposition. If, alternatively, a closed system was used, nitrogen pressure maintained at 10 atm and the temperature

---

[13] JANAF Thermochemical Tables, U.S. Government Printing Office, Washington, D.C., 1971.

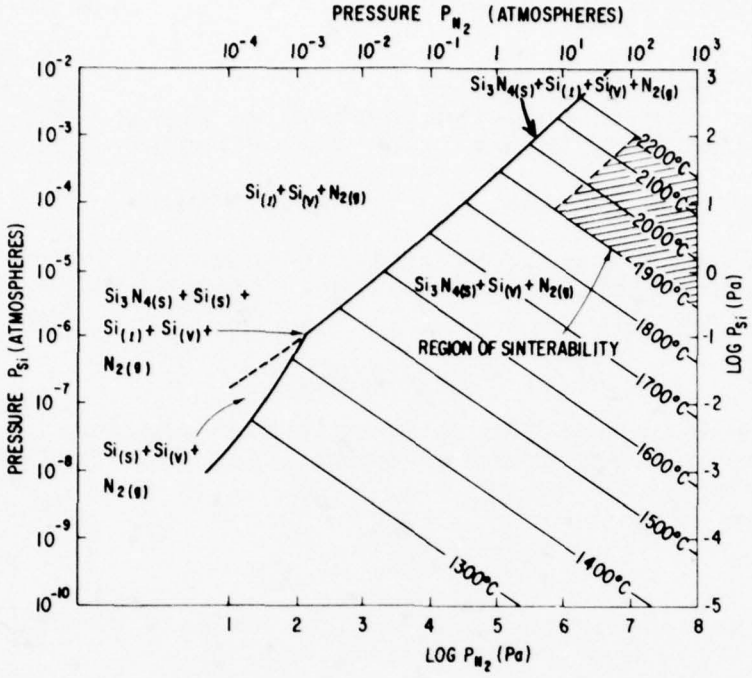

Figure 2. Silicon vapor pressure in equilibrium with silicon nitride as a function of nitrogen pressure and temperature.

gradually increased, silicon vapor pressure would increase (along vertical lines in Figure 2) until the liquid-solid coexistence boundary is reached where liquid silicon forms (univariant system). On further exposure all Si_3N_4 would isothermally decompose into liquid Si and N_2 and the rate of decomposition would be controlled by heat flow.

B. Silicon Vapor Barrier

From the above discussion it follows that two conditions have to be fulfilled to prevent decomposition of Si_3N_4 at high temperatures:

a. Nitrogen pressure has to be sufficiently high to keep the system to the right of the solid-liquid coexistence boundary, and,

b. Silicon vapor loss from the system has to be prevented.

As higher temperatures are used the second condition becomes increasingly critical as the rate of evaporation and vapor transport increase with temperature. This results in the requirement of isothermal confinement for the Si_3N_4 specimens by a wall impermeable to silicon vapor during the sintering operation.

There are only a few materials which may serve such purposes near 2000°C under nitrogen pressure - perhaps carbon, SiC, BN, AlN, B_4C, and silicon nitride itself. (Carbon would become siliconized at its surface and develop an impermeable SiC coating.) In the present experimentation we have selected SiC in the configuration of a closed end tube 1 cm I.D. which also serves as a pressure vessel.

Closed end tubes 25 cm long, approximately 1.15 cm O.D. and 1 cm I.D. in the final fired state, were slip cast from an aqueous dispersion of silicon carbide stabilized by tetramethylammonium hydroxide at pH 10 and 1/2% by weight of solid of urea-formaldehyde resol.* Slip casting was done in plaster-of-paris molds, and the castings were fired at 2150°C in one atmosphere of argon to a final density of 95%. The closed end of the tube is hemispherical and the wall thickness is about 1.5 mm.

Pressurizing of a thin walled, closed end tube results in tangential and longitudinal tensile stresses:

$$\frac{Pd}{2t} \quad \text{and} \quad \frac{Pd}{4t}$$

respectively, where P is the inside hydrostatic pressure, d is the diameter and t is the wall thickness.

The open end of the tube is sealed into a pressure head with epoxy resin and "proof-tested" at room temperature by pressurizing to 15 MPa nitrogen pressure which results in hoop stresses of approximately 52 MPa. The tube is inserted into a graphite resistance laboratory furnace of the type described by St. Pierre and Curran.[14] The entire assembly has been sketched in Figure 3, and a photograph of the tube sealed in the pressure head is included in Figure 4. Gas cylinders are used as the source of nitrogen and the pressure is controlled with a pressure regulator.

The temperature is measured by an optical pyrometer sighting on the closed end of the tube through a window in the opposite end of the furnace. By adjusting the position of the tube progressively farther into the furnace, it is possible to measure the temperature gradient near the hot zone and to position the tube such that the highest temperature is about 1 cm from the end. In this position there is a temperature drop from the hottest spot to the closed end of about 30°C and a total length of approximately 2 cm within 30°C of the maximum temperature. The temperature measured by the pyrometer has been

*URAC 180, American Cyanamide Co.

(14) P.D. St. Pierre and M.J. Curran, "A Simple Laboratory Furnace for Temperatures Up to 2500°C," General Electric Report No. CRD-012, December 1972.

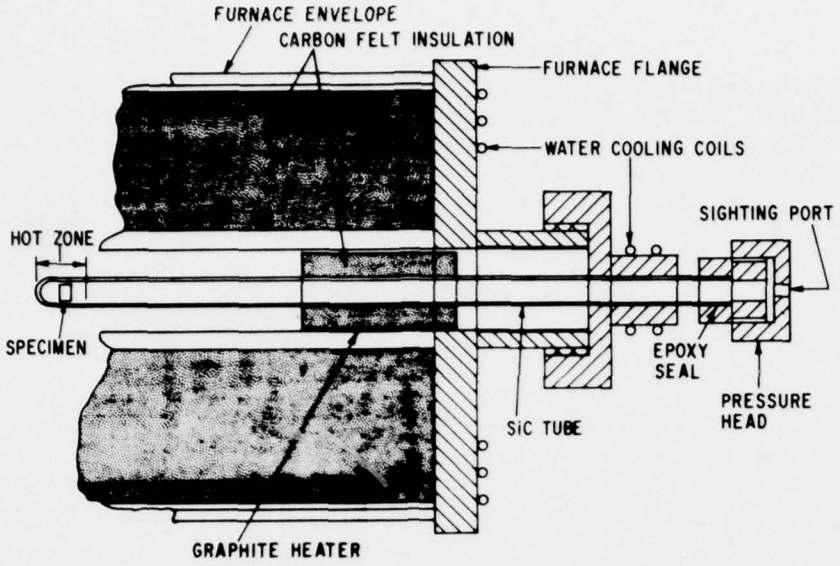

Figure 3. Schematic of furnace for sintering experiments with Si_3N_4 under nitrogen pressure.

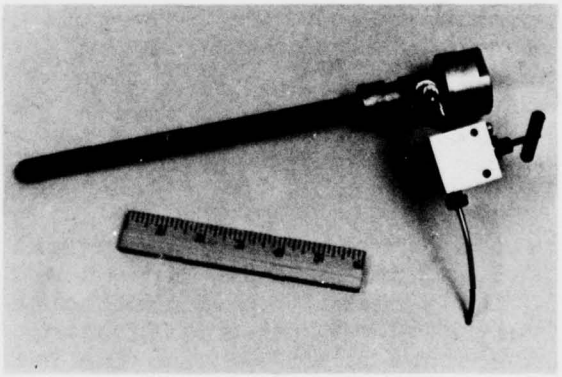

Figure 4. Silicon carbide tube and pressure head used for Si_3N_4 sintering work.

corrected for losses by the furnace window and a mirror, thus resulting in an estimated accuracy of $\pm 30^{\circ}C$ for all quoted temperatures.

During experimentation several tubes ruptured. In all instances the debris was safely contained within the furnace

envelope and no other damage occurred except to the heater and insulation.

C. The Relative Thermal Stability of SiC and Si_3N_4 Under Nitrogen Pressure

It is of interest to consider the relative stability of SiC and Si_3N_4 under high temperature and nitrogen pressure. This is best done by plotting the partial pressure of silicon above the two compounds as a function of temperature and nitrogen pressure. Such a diagram is shown in Figure 5. The parallel lines

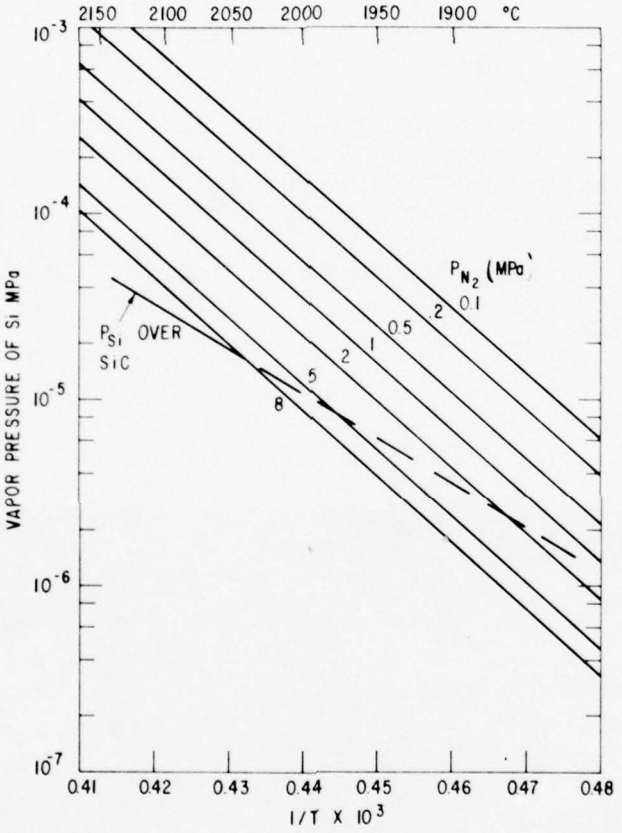

Figure 5. Silicon vapor pressure above Si_3N_4 and SiC as a function of temperature.

show P_{Si} over Si_3N_4 at various P_{N_2} in the temperature range of interest and the dashed line gives P_{Si} over SiC, according to Reference 15. The crossover points to the dashed line with the set of solid lines determines conditions under which SiC and Si_3N_4 have the same P_{Si} and are therefore stable. To the right of the crossover points SiC has higher P_{Si} and

(15) J. Drowart and G. DeMaria, "Thermodynamic Study of the Binary System Carbon-Silicon Using a Mass Spectrometer" in Silicon Carbide, J.R. O'Connor and J. Smiltens, eds., Pergamon Press, New York 1960.

should be, therefore, converted to Si_3N_4. The result also shows that under these conditions Si_3N_4 should be stable in contact with carbon. To the left of the crossover points SiC is stable in nitrogen, and Si_3N_4 would react with carbon (if present) to SiC. For 1 atm N_2 the diagram predicts an SiC-Si_3N_4 equilibrium temperature near 1500°C (not shown in Figure 5).

The essential point is that conditions exist under which Si_3N_4 will not react with carbon and that consequently a carbon resistor furnace and a carbon enclosure for the sintering objects are applicable. This is particularly important for temperatures considered here, where tungsten cannot be used due to silicide formation.

The conversion of SiC to Si_3N_4 predicted by the diagram in Figure 5 is so slow that it may be ignored for most of the conditions considered here. Nevertheless it has been observed. Figure 6 shows a section through a SiC tube which was exposed 7 hrs. at 2050°C at 8 MPa N_2. A thin layer of Si_3N_4 formed on the inner surface of the tube, and the rejected carbon is located in the large pores near the interface.

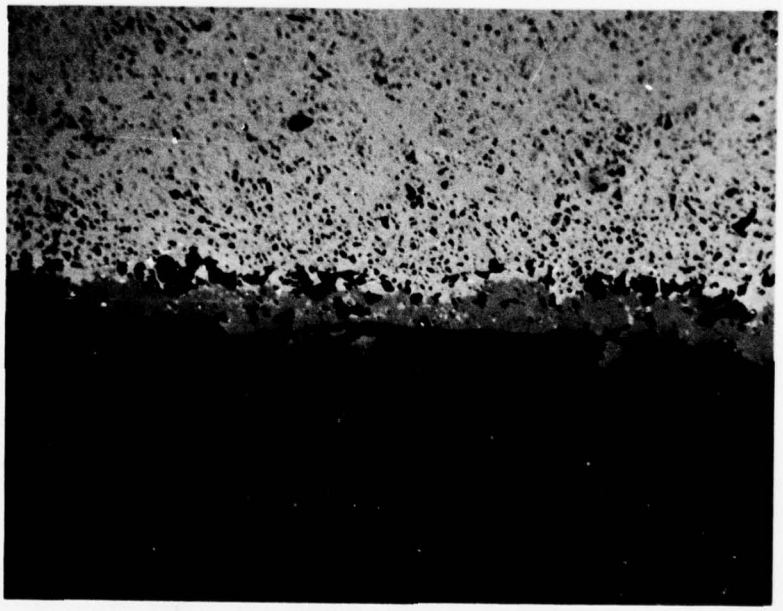

Figure 6. Silicon nitride layer formed on the inner wall of a SiC after exposure to 8 MPa N_2 at 2050°C for 7 hours. Mag. = 230X.

V. SILICON NITRIDE POWDERS

A. Selection of Powders

Previous work in this laboratory showed that the densification in covalent solids is more sensitive to impurities than in other ceramics. For instance 1/2% of free silicon or other metals will inhibit sintering of SiC dramatically and the absence of boron will turn off densification completely. Similar behavior was expected also in silicon nitride, and therefore a number of starting powders were selected to cover a wide range of chemical compositions. A very high purity powder was synthesized in-house from SiH_4 and NH_3 and was used in certain experiments. Additional powders were procured from vendors and characterized in the laboratory.

1. High purity Si_3N_4 from GTE Sylvania, grade SN-502 (60% crystalline + 40% amorphous). It is derived from $SiCl_4$ and, according to the supplier contains oxygen, chlorine, and traces of molybdenum.

2. Indussa Si_3N_4 standard grade, a product of Nippon Denko Co. Japan, a typical commercial, low priced crystalline powder of medium purity.

3. Silicon nitride - hot pressing grade, from H. Starck Inc. This has been specified as the highest purity of its kind, prepared by nitridation of silicon. The company developed a continuous process of nitridation and claims the lowest oxygen, free silicon and calcium content.

4. In-house amorphous Si_3N_4 prepared from SiH_4 and NH_3. It is very low in metals but contains variable amounts of oxygen and up to 2% hyperstoichiometric silicon. The preparation procedure was described before.[1] Its supply has been limited and is not expected to be used for larger specimen fabrication.

5. Electronic grade Si_3N_4 from Cerac Inc., which according to the supplier's information was expected to be predominantly the β form of Si_3N_4. Although this turned out not to be the case, its high purity and low oxygen content warranted meaningful experiments.

6. Indussa-low calcium grade Si_3N_4 - an experimental grade from Nippon Denko was also characterized and used in a few experiments.

B. Powder Characteristics

The powders were analyzed in the as-received form and the results together with other characteristics are summarized in Table 1. Oxygen has been determined by neutron activation, free silicon was estimated by X-ray diffraction (2% limit), surface area and density measured by low temperature nitrogen adsorption and helium displacement.

TABLE 1. CHARACTERISTICS OF Si_3N_4 POWDERS IN AS RECEIVED CONDITIONS

Supplier		GTE Sylvania	Indussa	Indussa	H. Starck, Inc.	Cerac Co.	Prepared In-House
Grade		SN-502	Standard	Low Calcium	Hot-Pressing	Electronic	--
Batch No.		--	51-7-1	Experimental	118	3263	22/23
Spectroscopy:							
PPM	Al	<30	4300	500	1800	700	<30
	Fe	<10	4000	2500	700	<30	<10
	Ca	<30	3000	200	1200	300	<30
	Mg	<40	--	100	300	40	<40
Other Elements		Mo, Cl	Mg, Na, C	Cr, Sb, Mn, Cu, Ni	n.d.	B, Ti	
Oxygen %		2.6	1.8	1.6	1.1	0.9	2.08
Carbon %		--	n.d.	0.4	0.6	0.0	--
Free Silicon est.%		0.0	4	n.d.	<2	<2	<2
Surface Area, m^2/g		5.0	2.6	6.0	7.8	7.0	9.5
Density		n.d.	3.14	n.d.	3.17	3.18	3.10
X-Ray α/β		95/5* 60% crystalline	50/50*	n.d.	90/7*	65/35	Amorphous

*Supplier's Information

C. Oxygen Content

All fine nitride powders, analyzed for oxygen so far, contain 1-3% O_2. Although some oxygen solubility in α-Si_3N_4 is very likely,[16] it is believed that a major fraction of the oxygen is present as a multimolecular layer on the particle surfaces similarly as has been found in silicon and AlN.[17] An upper limit of surface oxygen may be estimated from Table 2 which shows oxygen pick-up as a result of comminution and amounts to about 0.07% per m^2/g. Some oxygen may also be present as silica, as has been shown by Jack,[16] and in our previous work. Such oxygen can be removed by leaching with NaOH solutions or by reduction in an ammonia or hydrogen atmosphere between 1100-1300°C.[18] However, as will be shown below, there does not seem to be immediate need for very low oxygen levels in the starting materials as it forms a necessary constituent in the selected system. Oxygen concentrations near 2.5 wt%, similar to that found in many starting materials, are needed to bring about sintering.

D. Carbon Content

Si_3N_4 powders which originate from nitridation of silicon may contain certain amounts of carbon. See Table 1. Carbon is introduced in the process of preparation of silicon from silica and is, by all probability, present as SiC although usually below the detectability limit of current X-ray diffraction analyses.

To obtain positive proof of SiC, a sample of Si_3N_4 powder (Starck) was exposed to 1500°C in vacuum until it lost about 2/3 of its initial weight. SiC, being more stable under these conditions concentrated in the residue and was detected by X-ray diffraction.

As discussed above SiC may be either stable or could convert to Si_3N_4 at the sintering temperature depending on P_{N_2} applied. To determine whether or not there would be an effect of SiC on the sintering process, 5% of fine β-SiC ($8m^2/g$) was added to a composition prepared of in-house Si_3N_4 powder and sintered at 2080°C. No difference in sintered density, compared to powder without SiC addition was found indicating that small amounts of SiC would not interfere with Si_3N_4 sintering.

---

(16) S. Wild, D. Grieveson and K.H. Jack, "The Thermodynamics and Kinetics of Formation of Phases in the Ge-N-O and Si-N-O Systems," Special Ceramic, No. 5, Brit. Cer. Res. Assoc., Stoke-On-Trent, June 1972.

(17) H.G. Maguire and P.D. Augustus, "The Detection of Silicon-Oxynitride Layers on the Surfaces of Silicon-Nitride Film by Auger Electron Emission," J. Electrochem. Soc., 791-93, June 1972.

(18) T.R. Wright and D.E. Niesz, "Improved Toughness of Refractory Compounds," NASA Report No. CR-134690(1974).

TABLE 2. EFFECT OF MILLING AND ACID LEACHING ON CHARACTERISTICS OF Si_3N_4 POWDERS

Powder Origin	Internal Code	Sp. Surface Area(m^2/g)	Ca PPM	Fe PPM	Oxygen %	% Oxygen per m^2/g of new surface area
CERAC	CERAC	7.0	300	30	0.90	--
CERAC processed	CER B2	12.8	100	30	1.08	0.031
Indussa	"Low Calcium"	6.0	200	2500	1.60	--
Indussa processed	Ind. LCI	14.1	200	80	2.23	0.077
GTE Sylv.	SN-502	4.5	<40	<10	2.6	--
GTE Sylv. processed	SN-502-23A	13.3	<40	<10	3.2	0.068
H. Starck	Stk 118	7.8	1200	700	1.1	--
H. Starck processed	Stk 19A	14	600	30	1.47	0.06

E. Free Silicon

Si_3N_4 prepared by nitridation of silicon always contains residual silicon. It can be determined (after milling) by hydrogen evolution according to the reaction:

$$Si + 2KOH + H_2O = K_2SiO_3 + 2H_2$$

and may be removed in the same way. In the present work small amounts of finely dispersed silicon are of no concern as it is expected to convert to Si_3N_4 under the sintering conditions.

F. Powder Processing

Prior investigation of sintering of covalent solids - SiC, Si, B_4C[19] showed that favorable results were not obtained unless powders in the 0.1-0.3 micron particle size range were used. The same requirement was therefore extended to the present work.

[19] C.D. Greskovich, J.H. Rosolowski and S. Prochazka, "Ceramic Sintering," Final Report, 1975, General Electric SRD-75-084.

None of the procured powders was fine enough and most formed very coherent aggregates and had to be comminuted. Previous experience with SiC identified extended ball milling with steel balls (3/16") as a satisfactory procedure and was therefore adopted. It was done in a steel jar in hexane with charge to ball ratio of 1/5. The requirement was to obtain surface area of about 12 m^2/g which took between 70 and 100 hrs. of milling. Hexane was dried off and the residue leached with 5% HCl to remove iron wear from the milling media (2-5% Fe per charge). The ferrous chloride was removed by lengthy decanting while keeping pH of the aqueous dispersion at about 2 to prevent deflocculation. The final wash was done with acetone and the powder was recovered by filtering. It was observed that the leaching procedure removed the original content of iron and decreased, in some cases, the level of calcium. The effect of processing on the chemical composition of four Si_3N_4 powders is shown in Table 2.

Additional leaching experiments were done with KOH which resulted in an additional slight decrease of the oxygen level but did not affect other impurities. For instance, a caustic leach (following an acid leach) of the Starck powder decreased the oxygen level from 1.47% to 1.2%.

Our experience has been that crystalline silicon nitride is very stable, and current aqueous processing, such as used for alumina, is quite satisfactory. This is not the case with amorphous powders. These have been found to partly hydrolyze on exposure to moisture and to dissolve in dilute HF. Therefore, the in-house amorphous powder was not subjected to the described processing. This circumstance also suggests that caution should be taken with crystalline powders prepared by calcination from amorphous materials which may not be fully crystallized and the unconverted fraction would be suceptible to hydrolysis. This would be manifested by a substantial oxygen increase.

VI. SINTERING EXPERIMENTS

A. General

The objective of experiments discussed in this paragraph was to determine conditions for sintering of the selected Si_3N_4 composition to high density, say 95% of theoretical. The information sought was:

1. How do various Si_3N_4 powders respond to sintering with additions which were found effective previously and whether or not the response may be improved by processing of the powders.

2. How strongly changes of time, temperature, nitrogen pressure and green density influence sintered density.

3. What other factors, in addition, control final density.

Quantitative work was severely hindered by these latter factors which were only gradually recognized, i.e., oxygen level, oxygen loss during the sintering cycle and impurity transport. Although some parameters were not fully controlled and some experiments were not very reproducible, the observed trends discussed below are believed to be qualitatively correct.

B. Sintering Additives

Previous work showed encouraging results where Mg_3N_2 and Be_3N_2 were used as sintering additives, particularly when used in combination. Therefore the testing of sinterability of the new powders was done with the same additives. Be_3N_2 and Mg_3N_2 were purchased from Ventron Co., Beverly, Mass. According to the supplier, both were prepared by nitridation of metals and were 95 and 98% pure, respectively. All the batch formulations and powder preparation were done under glove box conditions to avoid hydrolysis due to atmospheric moisture.

To circumvent the inconvenience of working in a dry box, $BeSiN_2$ and $MgSiN_2$ were synthesized. These are stable compounds, do not hydrolyze even in water, and were used on an equivalent basis in formulation of compositions later in the work.[20,21]

$BeSiN_2$ has been prepared by mixing stoichiometric amounts of Be_3N_2 and Si_3N_4 in a mortar and firing the mixture in an SiC crucible at temperatures between 1800° and 2000°C under 2.7 to 8.2 MPa N_2 for 15 minutes. The product, a grey-white powder or friable aggregate, was analyzed by X-rays. Under all conditions $BeSiN_2$ was obtained with minor amounts (<10%)

---

(20) P. Eckerline, A. Rabenau and H. Nortmann, "Darstellung and Eigenschaften on $BeSiN_2$," Z.An u. Alg. Chem. 353, 113(1967)

(21) J. David and J. Lang, "Sur un nitrure de magnesium et de silicium," C.R. Acad, Sci. 261, 1005(1965).

of β-Si_3N_4. The detected Si_3N_4 may be either unreacted Si_3N_4 converted to β, or it may be a β' solid solution of beryllium oxide in Si_3N_4 resulting from a reaction with oxygen present.

$MgSiN_2$ was prepared similarly.

In some experiments the effect of oxygen additions via fine amorphous SiO_2 ("Cabosil," Cabot Co., Boston, Mass.) was studied.

C. Specimen Preparation

Processed powders were usually mixed with additions by mortar and pestle in about 2g amounts. Two percent of paraffin added in solution was used with some powders to improve pressing behavior. Alternately 25g batches were prepared by mixing in a plastic jar in a benzene dispersion using stearic acid as dispersant and silicon nitride milling media. Cylindrical specimens were die pressed at 28 to 70 MPa and then frequently repressed isostatically at 200 MPa. The final diameter of the green compacts was ~1 cm or 1.6 cm. Test bars 0.5 x 0.5 x 5 cm were die pressed similarly. Green density of the specimens from the processed powders was quite satisfactory, typically 58-61% of theoretical, except for SN-502 Si_3N_4 powder which would yield 48-51% (depending on the pressing pressure) and the In-House powder, which was not milled, yielding 46-48%.

In some instances the green specimens were prefired either in purified nitrogen of P_{O_2} $<10^{-6}$ or in air at 900°C. Air atmosphere was used to introduce additional oxygen into the composition. Table 3 gives the oxygen pickup calculated from the weight gain of a 1 cm x 1 cm cylindrical pill of Starck Si_3N_4 exposed to temperatures up to 1050°C and that found analytically. The exposure to air at 900°C for one hour results in 1.6% oxygen pickup and temperatures of 750°C or less do not bring about any measureable change in oxygen concentration. This latter finding is useful information in that it gives the upper limit of heat treatment one may use to burn out organic additives used in Si_3N_4 fabrication.

D. Firing of Specimens

Before sintering, a single pellet was inserted into the SiC tube (see above) and covered with loose Si_3N_4 powder. The use of pack powder to protect specimens during firing has been a common procedure in experiments with nitrogen ceramics and was also adopted early in the present work. It has been observed that the pack powder, under certain circumstances, may critically influence sintering and therefore a routine procedure was established, which has not been changed during experiments when other sintering parameters were investigated. This procedure has been to use a mixture of previously used pack powder with an addition of 1/4 to 1/3 of the

TABLE 3. OXIDATION OF Si_3N_4 IN AIR FOR ONE HOUR

T°C	ΔW/Wo%	Δ% O_2 Calc.	O_2 Determined*	Δ%O_2 Found
400	0.0	--	1.42	--
600	0.0	--	n.d.	--
700	0.0	--	1.67	0.0
800	0.12	0.30	n.d.	--
850	0.34	0.82	2.45	1.03
900	0.46	1.11	3.10	1.58
950	0.67	1.69	3.57	2.15
1000	1.03	2.45	n.d.	--
1050	1.34	3.18	n.d.	--

* Measured by neutron activation analysis

charge of fresh silicon nitride supplied by Apache Chemicals, Inc. cat. No. 6867 (Ca 500, Al 700, Fe 90, Mg 50, Cr 20, O_2 14000, C 2000 in PPM). The reason for this selection and procedure has been that it would yield best density results and, secondly, that this pack powder was easily removed from the tube or crucible after firing.

A typical sintering schedule involved heating up in vacuum to 800°C, holding for about 5 minutes to remove the binder, pressurizing the SiC tube with nitrogen and heating in about 5 minutes to the sintering temperature ("fast heating rate") or alternatively in about 20 minutes ("slow heating rate"). After every run the O.D. of the tube was measured and when creep strain exceeded 4% the tube was replaced to avoid subsequent catastrophic rupture. The firing procedure in the autoclave described below, was essentially the same except that a slower heating rate was used and the specimens, usually

several at a time, were placed in a silicon carbide crucible 2.5 x 2.2 x 15 cm.

A high-pressure high temperature furnace, with capabilities applicable in present work, was designed and built in this laboratory. The basic design features were derived from a controlled atmosphere furnace by St. Pierre and Curran.[14] It uses a graphite foil (Grafoil, Union Carbide Co.) heating element 12 inches long, easily replaceable, and may be operated at up to 2300°C at 100 atm of inert gas pressure (inert with respect to carbon) and has a hot zone of 2.5 x 7 cm. A photograph of the furnace appears in Figure 7. Overheating of the end flanges and incorrect temperature read out through a sighting port were major difficulties encountered in the initial use of this furnace. The first was overcome by redrilling more efficient cooling channels and by providing water cooled end covers. The temperature measurement was a more difficult problem to solve.

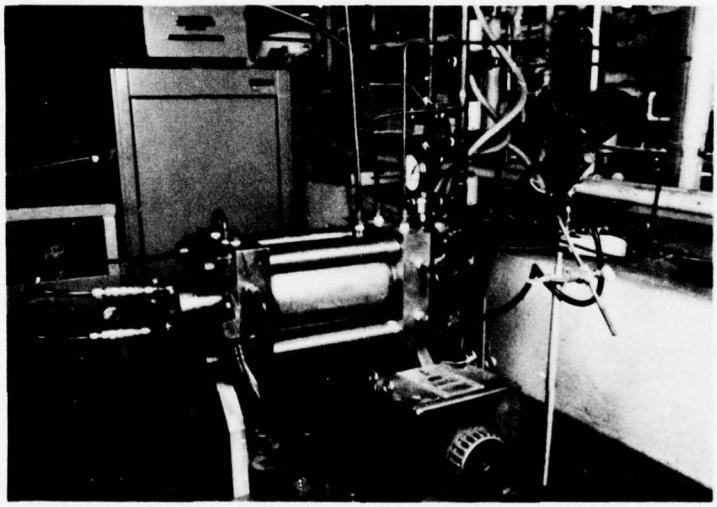

Figure 7. Autoclave for sintering under gas pressure up to 8 MPa and 2300°C. 2 1/2 x 7 cm hot zone.

The design of the furnace called for optical temperature determination axially through a sighting port in the end cover. However, the density gradient in the pressurized gas (due to temperature gradient in the furnace) severely defocuses the light from the target so that a large pressure dependent deviation in the read out results. As shown in Figure 8 the apparent temperature read by an L&N optical pyrometer at the melting point of alumina is a strong function of N_2 pressure and at 7 MPa a correction of 300°C would be necessary. Moreover, above about 1700°C the apparent temperature vs. true

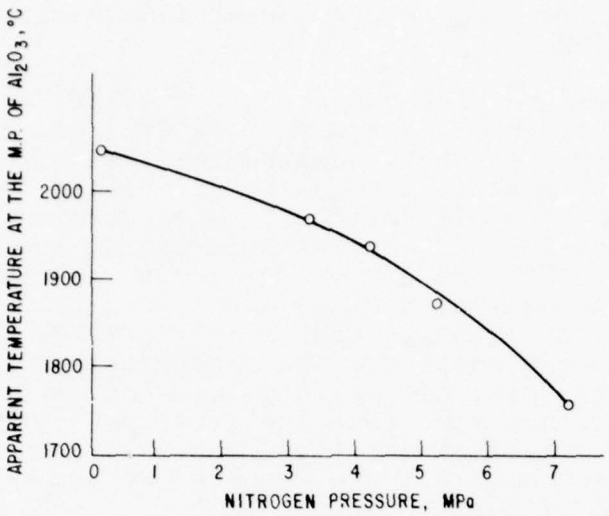

Figure 8. Effect of nitrogen pressure on apparent temperature read by an optical pyrometer in the autoclave.

temperature curve is so flat that correcting the apparent temperature is not a viable way to measure temperature. The problem is further compounded by fogging of the sighting port. In addition, attempts to calibrate the power setting at the melting point of alumina was not useful as the power setting at a temperature depends on gas pressure in the furnace, the length of the crucible holding the specimens and aging of the heating element.

The solution to the problem was obtained by redesigning one end of the furnace so that a closed end silicon carbide tube 0.75 x 1.0 x 13 cm could be sealed with the open end into the sighting port and its bottom near the hot zone providing a target for optical temperature read out. The design is shown on Figure 9. The pyrometer was calibrated at the melting point of sapphire observed through the other sighting port. The temperature reading is believed accurate within $\pm 20^{o}C$.

E. Specimen Evaluation

Weight loss, shrinkage and displacement density were obtained by usual procedures. The specimens, small cylinders, were frequently tapered, and sometimes flared towards both ends, due to nonuniform shrinkage. In this case longitudinal shrinkage, or average radial shrinkage was used. Most of the specimens were sectioned and polished to investigate pore size and porosity distribution. Some were further studied by X-ray, optical microscopy after etching, SEM and TEM. These investigations are reported below.

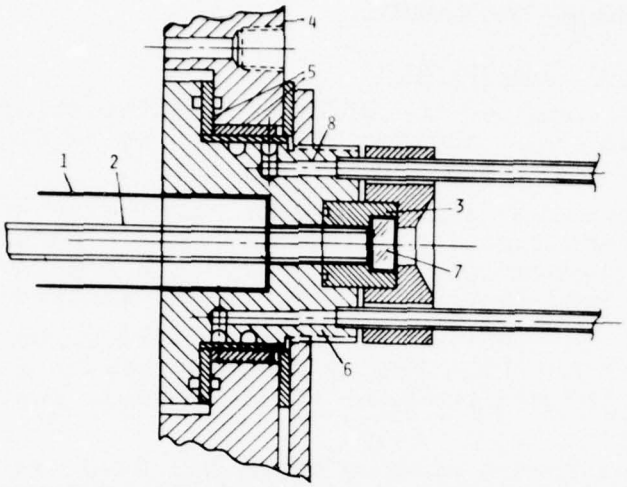

Figure 9. Sighting port of the autoclave after redesign: 1. Grafoil heater, 2. Closed end SiC tube sealed in, 3. Tube holder, 4. Furnace flange, 5. Teflon insulation, 6. Rear electrode, 7. Quartz window, 8. Cooling channel.

VII. RESULTS OF SINTERING EXPERIMENTS

A. Effect of Composition

Table 4 compares the effect of additions of Mg_3N_2, Be_3N_2 and combination of the two on fired density of four Si_3N_4 powders. The results reveal that:

1. Magnesium nitride is only marginally effective in promoting densification. This may be, in part, the consequence of evaporation of Mg_3N_2 from the specimens. Analysis of one sintered specimen found 0.4% Mg instead of 1.5% added.

2. The combination Be and Mg nitrides has been very effective with the high purity in-house powder and both with Starck and Indussa powders; SN-502 powder, however, did not respond well.

3. Even in the absence of Mg_3N_2, Be_3N_2 is effective enough to bring about densification if its concentration and other conditions were optimized.

Based on this later finding, we decided to omit Mg_3N_2 from the composition in the succeeding experiments. The decision was stimulated by preliminary oxidation tests which showed substantially accelerated oxidation in specimens containing Mg compared with specimens hot-pressed with Be addition only. The poor response of the SN-502 was corrected in later experiments by a specific firing schedule including prefiring of the specimens at 1350-1450°C in vacuum prior to sintering. The nature of the different behavior of this powder is not clear; perhaps it is related to residual chlorine content which is specific for this powder. A chlorine-containing hygroscopic compound was identified in a deposit formed over this powder by heating at high temperature on several occasions.

Table 5 shows the effect of varying Be concentration on the in-house Si_3N_4 powder (added as Be_3N_2) and the Starck-118 powder, both as received and milled to $14 m^2/g$ (Be introduced as $BeSiN_2$). In all three experiments it appears that a specific concentration exists for each powder which allows maximum sintered densities. A similar observation was done previously in a study of hot pressing Si_3N_4 with Be_3N_2 additions.

In experiment No. 81 a final density of 92% was achieved with 0.5% Be addition (3.5% $BeSiN_2$). This composition was reinvestigated in more detail and the results are shown in Table 6. Again a 0.5% Be addition maximized final density. The sintered density, however, could not be increased above 92% by increasing temperature because "bloating" occurred above 2100°C (manifested by convex curvature of the pellet's faces) and resulted into large pore formation. Nevertheless the local density in specimen No. 87 was high, probably above 95%. The data also show that densification just

TABLE 4. RESPONSE OF DIFFERENT Si_3N_4 POWDERS TO SELECTED SINTERING ADDITIVES: SINTERED DENSITY %/WEIGHT LOSS %

$T°C/P_{N_2}$, MPa	2% Mg_3N_2	2% Be_3N_2	1% Be_3N_2+2%Mg_3N_2
In-House Si_3N_4 - Green Density 46%			
2000/8	63.47	74/5.4	92/4.5
2050/8	--	80/5.7	94/5.5
2100/8	66/8.0	86/5.7	93/8.1
Indussa Si_3N_4 - Green Density 61%			
2000/7.5	81/1.5	72/1.5	92.5/1.0
2050/7	82/-	82/2	93/-
2080/7	--	84.5/2	--
Indussa Si_3N_4 Milled - Green Density 53%			
1880/7.5	--	--	94/1.9
1930/7.5	--	--	93/2.4*
2020/7.5	--	--	93/4.5*
SN-502$^+$ - Green Density 48%			
2000/7.5	--	84/5.9	75/4.0
2000/9.5	59/7.4	--	--
2050/7.0	61/-	95/5.9	75/4.6
2080/9.5	--	94/5.7	--
Starck - Green Density 61%			
Milled 2000/8.2	--	86/2	91/2.5
2050/8.2	--	92/2	94/2.5
2080/8.2	--	92/3.5	--

TABLE 5. EFFECT OF Be CONCENTRATION

Exp. No.	% Be	T°C/P_{N_2}, MPa	Fractional Density % / Weight Loss %	Comment
Si_3N_4 Synthesized In-House, 46% Green Density				
17	0.25	2050/7.1	50/3.7	Be added as Be_3N_2
16	0.50	2100/7.1	64/5.5	
22	1.0	2100/7.1	86/5.7	
20	2.0	2100/7.1	69/7.3	
Si_3N_4 Starck-118, as received, 61% Green Density				
75	0.15	2100/8.2	63/-	Be added as $BeSiN_2$
74	0.5	2100/8.2	77/3.4	
73	1.0	2100/8.2	75/1.8	
Si_3N_4 Starck-118, milled+, 60% Green Density				
82	0.3	2100/8.3	83/1.4	Be added as $BeSiN_2$
81	0.5	2080/8.2	92/3.7	
77	1.0	2100/8.2	88/3.0	
Si_3N_4 SN-502, 48% Green Density				
65	0.5	2100/8.3	74/5	Be added as $BeSiN_2$
61	1.0	2080/8.3	90/5.5	

* No. corresponds to in-house log.

\+ 14 m^2/g

TABLE 6. SINTERING OF Si_3N_4 - STARCK (MILLED) + 0.5% Be

Experiment No.	% Be	T(°C)/P_{N_2} (MPa)	Fractional Density %	Weight Loss(%)	Comment
Effect of Be					
85	0.13	2080/8.2	82	1.1	Fast
82	0.27	2080/8.2	83	1.4	Heating
81	0.50	2080/8.2	92	3.7	Rate
77	1.00	2100/8.2	88	3.0	
Effect of Nitrogen Pressure					
--	0.5	2080/1.3	--	--	Total decomposition
84	0.5	2080/2.75	90	11.6	Substantial fraction of free Si.
83	0.5	2080/5.5	91	--	
81	0.5	2080/8.2	92.5	3.7	
Effect of Sintering Temperature					
101	0.5	1800/7	65	2.0	
92	0.5	1950/8.2	79	2.0	
86	0.5	2050/8.2	91.7	3.4	
81	0.5	2080/8.2	92.4	3.7	
87	0.5	2120/8.2	90	3.9	Specimen bloated, local density >95%

about starts at 1800° at which point 2% linear shrinkage was measured (exp. 101).

Also in Table 6 is shown the effect of nitrogen pressure on sintered density at 2080°. At 1.3 MPa N_2 the specimen completely decomposed. Calculations show that for 1.3 MPa N_2 the equilibrium temperature would be 2130°, i.e., 50° above the temperature measured, a fair agreement considering the uncertainty in temperature measurement and of thermochemical data. At 2.7 MPa 90% density was achieved. However, a substantial amount of free silicon, about 10%, was revealed in specimen No. 84 (Figure 10) and a substantial weight loss resulted (11.6%). The origin of this silicon is not quite obvious; it is perhaps related to interaction with impurities in the specimen. It is unlikely that the discrepancy with thermochemical calculation would be that large. In addition, no free silicon formed in the packing powder.

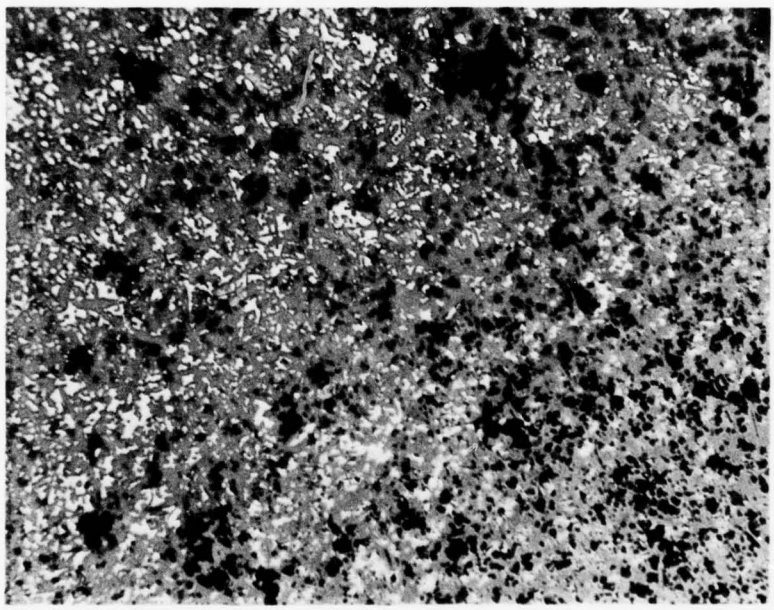

Figure 10. Microstructure of a Si_3N_4 specimen sintered at 2080°C and 2.7 MPa of N_2. (Notice substantial fraction of free silicon.) Mag. = 230X.

The result of the latter experiment contains additional information. Firstly, silicon metal does not inhibit densification of silicon nitride (contrary to SiC). Secondly, sintering close to the coexistence boundary is uncertain and may result in partial decomposition for reasons yet to be investigated.

In experiments 81 and 83 no free silicon formed, and consequently one can estimate the minimal necessary N_2 pressure to sinter at 2080° to be about 4 MPa. It is further observed that the increase of nitrogen pressure from 5.6 to 8.2 MPa increased the density only marginally if at all. Some experiments were repeated many times under nearly identical conditions and a substantial variance in the degree of densification was observed. Thus, final densities obtained in one composition of Starck Si_3N_4 powder varied between 85 and 95% and in SN-502 between 88-95%. An even greater variation was found in the processed Indussa powder where a composition with 1% Be yielded densities of 67% and 93% in two successive runs differing only in heating rates. These results could not be correlated to temperature, time, gas pressure or specimen green density and, clearly other variables were interfering. Highly suspect are impurity effects.

B. Effect of Heating Rate

A possible effect of heating rate was investigated in a series of experiments done with three powders. Changes in heating rates were introduced at 800°C, after the furnace was pressurized with N_2; "slow" 60°C/min or "fast" 250°C/min. The results collected in Table 7 show variations which cannot be correlated with heating rate. In additional experiments a soak for one hour at 1900°C was applied without a substantial difference in sintered density. It was concluded that no systematic effect of heating rate could be detected.

C. Effect of Oxygen

An effect of oxygen content was first observed in hot-pressing carried out with the in-house synthesized Si_3N_4 powder with additions of 7% $BeSiN_2$. These experiments showed repeatedly that a batch of powder containing 3 wt% oxygen hot-pressed easily to theoretical density at 1780°C while another batch containing 2% resulted in final densities of 85 and 88% at 1780°C and 1830°C.

A batch of powder, "Starck 118," was milled and leached successively with HCl and KOH to reduce the oxygen content from 1.9% to 1.26%. A composition with 3.5% $BeSiN_2$ prepared from this powder (STK-19B) showed little densification under typical sintering conditions (Table 8). When the powder or the pressed pellets were prefired in air at 900°C the sintering response was restored, strongly indicating that a certain oxygen content is essential to sinter the present Si_3N_4 composition. The "addition" of oxygen due to prefiring in air

TABLE 7. EFFECT OF HEATING RATE

Exp. No	%Be*	T°C/P_{N_2}, MPa	Density %/ Weight Loss%	Heating Rate**
In-House Si_3N_4, Green Density 46%				
52	1.0	2050/8.2	91/2.4	Slow
51	1.0	2050/8.2	94/3.8	Fast
69	1.0	2100/8.2	93/4.6	Fast
Indussa Si_3N_4(milled), Green Density 55%				
64	1.0	2050/7.5	88/4.6	Fast
65	1.0	2050/8.2	67/7.0	Slow
70	1.0	2100/8.2	93/4.9	Fast
SN-502 Si_3N_4, Green Density 48%				
65	1.0	2050/8.2	74/5.1	Fast
62	1.0	2050/8.2	90/6.8)	Slow up in vac. up to
61	1.0	2080/8.2	90/8.3)	1450°C, hold for 15 min. and fast to sintering temp.
132	1.0	2080/6.2	91/1.0	Prefired at 1350°/fast HR
133	1.0	2100/6.2	89.5/1.9	" slow
135	1.0	2100/7.5	98/1.5	" slow
136	1.0	2100/7.5	94/0.9	" slow
139	1.0	2100/7.5	89/0.8	" slow

*Be added as $BeSiN_2$

**Slow Heating Rate: 60°C/min

Fast Heating Rate: 250°C/min

TABLE 8. EFFECT OF OXYGEN ADDITION ON SINTERING OF Si_3N_4 - POWDER STK - 19B

Exp. No.	Addition wt.% $BeSiN_2$	Addition wt.% O_2	Pressed Density %	Sintering Conditions T°C/P_{N_2} (MPa)	Fired Density Weight Loss %/%	Comments
111	3.5	1.26%	60	2100/5.6	72 0.7	--
113	3.5	"	60.5	2120/6.3	76 0.4	--
114	3.5	"	60.5	2100/6.3	75 /0.5	Up to 1500°C in argon
115	3.5	"	58	2100/6.3	78 /-1.0	--
116	3.5	2.7%	60	2100/5.6	89 /2.0	Pellet exposed in air at 900°C/1h.
118	3.5	"	60	2100/5.6	92.5/2.0	+Pack powder oxidized
119	5.0	"	52	2100/5.6	87 /6.8	Powder exposed at 900°C
121	5.0	"	53	2020/5.6	85 /4.0	in air
122	5.0	"	60	2100/5.6	91 /1.4	Pellet exposed at 850°
123	5.0	2.3%	60	2100/5.6	91 /1.5	in air
124	5.0	"	60	2100/5.6	94.5/0.7	+Pack Powder oxidized

(Table 8) was determined by neutron activation analyses and was higher by about a factor of 1.5 from that determined from weight gain. This correction factor was applied in determining the actual oxygen concentration.

A similar study was done with three more powders - SN-502-23A, Cerac-B2 and Indussa -LC1 which had an oxygen content 3.2%, 1.08% and 2.23%, respectively. (See Table 2 for other characteristics.) About 1.5% oxygen was introduced in some of the experiments either by prefiring in air at 900°C or by adding 3% SiO_2 to the composition. The specimens were sintered at identical conditions at 2100°C in 6.0±0.5 MPa N_2 for 15 min. The results presented in Table 9 suggest the following conclusions:

TABLE 9. EFFECT OF OXYGEN ON SINTERING* OF Si_3N_4 POWDERS

Exp. No.	Powder Code	Base Oxygen %	Additions $BeSiN_2$ %	Additions SiO_2 %	Prefiring Conditions **		Weight Loss + %	Final Density %	Comment
136	SN-502 23A	3.2	7	--	1300°	N_2	0.9	94.3	
139	"	3.2	7	--	900°	N_2	0.8	90	
140	"	3.2	7	--	1050°	N_2	0.6	94.5	
143	"	3.2	7	--	900°	air	1.7	93.5	
133	"	3.2	7	1	900°	N_2	1.0	89.3	
129	Cerac B2	1.08	5	--	900°	N_2	0.0	72	
130	"	1.08	5	--	900°	air	0.0	81	
141	"	1.08	7	--	900°	air	0.1	81.5	
144	"	1.08	7	3	900°	N_2	0.5	91.6	
146	"	1.08	7	3	900°	N_2	1.4	92.5	Held 1 hr at 1900°C
137	Ind LC1	2.23	5	--	900°	N_2	0.8	80	
138	"	2.23	5	--	900°	air	0.4	86	
147	"	2.23	5	2	900°	N_2	1.5	86	
149	"	2.23	7	--	950°	N_2	0.7	85	
148	"	2.23	7	2	950°	N_2	0.4	86	

*All specimens sintered at 2100°C-15 min at 6±0.5 MPa N_2

+Weight loss based on prefired weight of specimen

**Purified nitrogen used, <1PPM oxygen; prefiring in air at 900°C introduces 1.0 - 1.5% oxygen

1. If the starting Si_3N_4 powder contains more than 2% oxygen, a proper amount of $BeSiN_2$ addition permits sintering to a density of 90% or higher. Such powder does not respond to further increase in oxygen content either introduced as SiO_2 addition or by exposing specimens to air at 900°C before sintering.

2. When the starting oxygen content is low, near 1%, an increase in oxygen aids densification substantially.

In view of the above results, which showed that small amounts of oxygen are critical for the sintering of Si_3N_4, it was conceived that the loss of oxygen during firing might account for the different sintering results obtained in the laboratory tube furnace and in the autoclave. Such possibility was inferred from higher weight losses on sintering in the autoclave and other observations such as the strongly inhibiting effect of free carbon on densification. Oxygen analyses of sintered specimens confirmed the loss of oxygen as shown in Table 10. Comparing exp. Nos. 136 vs. 152 and 144 vs. 154 one sees that final density correlates to final oxygen content and that firing in the autoclave did result in a substantial decrease of oxygen content. This evidence does not, however, prove that sintering was indeed inhibited by the oxygen loss; the oxygen may have been lost as a consequence of the specimen remaining porous at high temperature for other reasons.

D. Effect of Carbon Monoxide

A major difference between the sintering conditions in the SiC tube furnace and in the autoclave is that in the latter the sintering atmosphere is also in contact with the carbon heater. Consequently, if carbon was transported by some mechanism, strong inhibition of sintering could be expected. Carbon monoxide was first suspected as a possible transport medium for carbon. Small amounts of CO are always present in the furnace atmosphere due to oxygen in nitrogen and other sources.

In analyzing the effect of CO it is possible, to a first approximation, to ignore minority species in the gas phase, such as $(CN)_2$, Si, Si_2C, CO_2 and SiN and also carbon as a solid and base a thermodynamic analysis on the following reactions:

1. $2Si_3N_4 + 3CO = 3SiC + 3SiO + 4N_2$

2. $3SiO + CO = SiC + 2SiO_2$

3. $Si_3N_4 + 2CO = 2SiC + SiO_2 + 2N_2$

Reaction (3) gives the overall reaction of (1) and (2) combined. The equilibrium constant is then:

TABLE 10. EFFECT OF MODE OF FIRING ON THE OXYGEN CONTENT IN SINTERED SPECIMENS

Exp. No.	Composition and Powder Code	Starting % O_2	Sintering Atmosphere*	Final Density	Final % O_2
136	SN-502-23A + 7% $BeSiN_2$	3.2	Tube fnc. 6 MPa N_2	94.3	2.88
152	Same	3.2	Autoclave 6.5 MPa N_2	72	1.20
163	Same	3.2	Autoclave 5.5 MPaN_2 + 1.05 MPa CO	87	2.11
144	Cerac B2 + 7% $BeSiN_2$+3%SiO_2	2.6	Tube fnc. 6 MPa N_2	91.6	2.64
154	Same	2.6	Autoclave 6.5 MPa N_2	83.4	1.86
161	Same	2.6	Autoclave 5.5 MPa N_2 + 1.05 MPa CO	91.5	2.44

*Sintering runs made at 2100°C for 15 min. heating rate in the tube furnace 180°/min and 50°/min in the autoclave.

$$K = \exp(-\Delta G_3/RT) = \frac{P_{N_2}^2 \cdot a_{SiO_2}}{P_{CO}^2}$$

where a_{SiO_2} is the activity of SiO_2 in the solid solution, i.e., in Si_3N_4 . 2 x BeO · x SiO_2. Thus thermodynamics predicts, at least by this very simplified approach, that CO is not likely to promote removal of oxygen and that a specific pressure ratio of nitrogen to carbon monoxide exists at each temperature to bring the system to equilibrium. Thus carbon monoxide is expected to retard oxygen removal from Si_3N_4 by the formation of SiO and subsequent reaction with more CO to make SiO_2. Table 11 gives calculations of the pressure ratios and K for several temperatures and for SiO_2 activities of 1 and 0.1.

TABLE 11. EQUILIBRIUM CONSTANTS AND EQUILIBRIUM P_{N_2}/P_{CO} FOR REACTION 3

T(°K)	K	P_{N_2}/P_{CO}	
		$a_{SiO_2}=1$	$a_{SiO_2}=0.1$
2000	1.96	1.4	4.3
2100	1.62	1.27	4.0
2200	1.36	1.17	3.69
2300	1.17	1.08	3.41
2400	1.014	1.01	3.19
2500	0.892	0.94	2.97

Sintering experiments were conducted under CON_2 atmospheres both in the tube furnace and in the autoclave. Atmospheres containing CO (up to 1.4 MPa CO and P_{N_2}/P_{CO} = 4) did not interact with Si_3N_4, did not inhibit sintering and did retard oxygen loss as shown in data of exps. 161 and 154 in Table 11. In several instances CO containing atmospheres were beneficial to densification (density increased a few percent) but in general the effect was small. Inspection of polished sections of specimens sintered under CO pressure revealed the presence of grains of a new phase at a 1 to 2% level which, judging from reflectivity and etching behavior, was SiC. X-ray diffraction analysis of this same sintered specimen revealed a weak but distinct peak corresponding to β-SiC, in agreement with reaction 3.

E. Effect of Impurities

A number of indirect observations have been accumulated during this study to indicate that in addition to the oxygen and Be level, trace amounts of some species assisted the densification and that these species were transported through the sintering atmosphere and by the pack powder. These observations include the following:

a) The least pure powders (Indussa-Standard and Starck) sintered most consistently and required a lower level of additions.

b) The densities obtained on sintering in pure pack powders were always lower than those of specimens sintered in the currently used pack powder (see above).

c) It was observed that the side of a pure pellet (SN-502) which was facing a pellet of Indussa LC1 powder during sintering achieved a relatively high density (>90%) while the reverse side was more porous, with density near 80%.

d) Specimens from Cerac powder (with addition of 7% $BeSiN_2$ and 3% SiO_2) could be sintered to 94% without pack powder in presence of specimens pressed from Starck powder but achieved only 82% when fired under the same condition in combination with specimens from SN-502 powder.

e) Processed Starck powder without further additions achieved a density of 82% when hot-pressed under nominal conditions while pure powders did not respond at all.

f) In a sequence of sintering experiments it was observed that the densities of specimens of pure powders fired just after specimens of less pure powders were substantially higher.

More direct evidence of impurity transfer was obtained from the following experiment. The SiC tube was replaced with a new one cleaned with HNO_3 to exclude contamination. A specimen of SN-502 powder with 7% $BeSiN_2$ was then sintered at 2080/6.5 MPa/15 min. in fresh pack powder (Ca 500, Al 700, Fe 90, Mg 50, Cr 20, O_2 14,000 in PPM). The density was 82%. The experiment was repeated to yield 84%. In a third experiment a mixture of the above pack powder and Indussa Standard (Ca 3000, Al 4300, Fe 4000, O_2 18000) powder in a 1:1 ratio was used to cover the specimen. The density achieved under the latter conditions was 95%. The specimen when sectioned showed a dense periphery and a more porous core, Figure 11. This is most likely explained by assuming diffusion of a sintering promoting species inward from the surface. X-ray fluorescence analysis however did not reveal a compositional difference between the periphery and the interior, although a week signal for Ca was detected.

A similar experiment was carried out in the autoclave with with pills pressed fron SN-502 and Cerac-B2 both with 7% $BeSiN_2$ addition. The first run was made without pack powder and the second run with the impure mixed pack powder of the composition described above. The data in Table 12 give results of spectrochemical analysis of the sintered pills and shows clearly that metal concentration increased substantially, particularly Ca and to a lesser degree Mg and Fe, on sintering in the presence of impure pack powder.

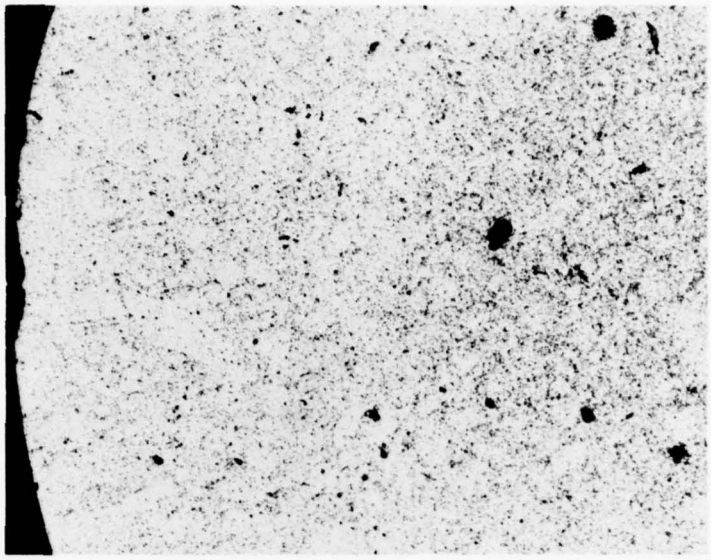

Figure 11. Section of sintered specimen of Si_3N_4-SN-502 + 7% $BeSiN_2$, showing dense periphery and more porous core presumably due to impurity transport from pack powder to the specimen.

In light of the above observations it appears that small amounts of metals, particularly Ca and probably Mg and Fe, promote densification of Si_3N_4 composition with Be additions and may be essential for achieving high densities (>90%) at the selected level of Be addition. These metals are readily transported through the sintering atmosphere probably well below the current firing temperature. In our experiments the source of the impurities has been the pack powder or the firing crucible or tube which collected impurities during previous use with less pure specimens and actually served as a reservoir for impurities.

During the firing cycle specimens may either accumulate or lose active impurities depending on the relative activity of these species in the source and in the specimens, and also on the rate of dissipation of the species out of the atmosphere in the hot zone. Thus, depending on these subtle circumstances a substantial variation in densification behavior may result.

Consider for instance the effect of oxygen in Si_3N_4, which is, most likely, the factor which determines activity of the impurities. The higher the oxygen content the lower their activity. If the oxygen level in the specimen is such that the activity of minority species is less than in the pack powder, the specimens will pick up impurities and sintering will be enhanced. If the opposite is the case, impurities will be transferred in the reverse direction, i.e.,

TABLE 12. IMPURITY TRANSPORT DURING SINTERING OF SPECIMENS IN THE AUTOCLAVE

Starting Powder Code		Cerac B2	SN-502-23A
Addition		7% $BeSiN_2$ 3% SiO_2	7% $BeSiN_2$
Sintering* Conditions		2080°C 6 MPa N_2 1 MPa CO 15 min	Same
Sintered Density		94%	89.5%
Starting Impurity Concentration PPM	Ca	100	<40
	Fe	30	<10
	Al	700	<30
	Mg	40	<40
Impurity Concentration in Sintered Specimens PPM	Ca	850	750
	Fe	150	100
	Al	800	<40
	Mg	150	80

*Impure pack powder used; approximate impurity content PPM: Ca 1500, Fe 2000, Al 2200

they will be lost from the specimens and consequently sintering will be inhibited. As the oxygen content in the pack powder is close to that in the specimens very small changes may result in the reversal of the trends. It is believed that the observed variability of sintering results has been a consequence of a similar situation.

Other factors may further compound this problem. If the specimen is large with respect to the volume of the hot zone and the loss of the impurities out of the hot zone atmosphere is small, the atmosphere composition (with respect to impurity concentration) will be dominated by the specimen composition. If the specimen is small other factors will control the impurity concentration of the atmosphere and hence the sintering process. It is our opinion that this has been the origin

of the differences in results of sintering in the tube furnace and the autoclave.

Oxygen loss from the specimens will be another controlling factor. As explained above, oxygen is assumed to control the activity of the impurities and therefore one may expect that oxygen loss will be coupled to the loss of the impurities in reducing environments.

The species actually transported are with all probability volatile nitrides (Ca_3N_2 and Mg_3N_2) which form from oxides due to the strongly reducing conditions of the sintering atmosphere. Preliminary results indicate that aluminum, which does not form a volatile nitride, has not been transported.

F. The Mechanism of Sintering in the Si_3N_4 - Be_3N_2 System

The absence of densification and sintering in many substances is related to rapid growth of particles (grains) and pores by mass transport along surfaces or through the gas phase. This process, designated as coarsening, is a consequence of the elimination of small pores and small particles while larger ones grow. The growing particles are usually not single crystal grains but pore-free domains composed of many grains.

It can be shown that many crystalline materials may be sintered at a temperature where D/d^3 (D the diffusion coefficient of the sintering rate controlling species, $D_o e^{-Q/RT}$, and d, the effective particle size) is near unity. If, however, d can grow by another mass transport process, it is possible that the above ratio never approaches unity with increasing temperature and consequently such materials will not densify appreciably. This is precisely the case with many covalent solids[22] and probably Si_3N_4 too.

Considering the above sintering criterion one sees that in order to promote densification one has to increase D, i.e., internal mass transport, reduce d and prevent or retard its growth (particularly at temperatures where internal mass transport is too slow to operate).

A well known example of an effect of increased diffusivity on sintering, mentioned above, is UO_2. When the concentration of uranium vacancies is increased due to reduction in the U/O ratio, "sinterability" is enhanced dramatically. An example of control of surface mass transport is perhaps the effect of boron in the sintering of SiC which,

---

(22) C.D. Greskovich and J.H. Rosolowski, "Sintering Covalent Solids," J. Am. Cer. Soc., 59, 336(1976).

according to Greskovich and Rosolowski,[22] retards surface mass transport.

The observation of the effect of oxygen in the sintering of Si_3N_4 with Be additions may be interpreted in similar terms. The formation of solid solutions in the system Si-Be-N-O is brought about by simultaneous replacement of two nitrogen atoms by two oxygen atoms for each Be atom going into a silicon site. It may be expected that the two oxygen atoms on nitrogen sites, each having one excess electron, will remain associated with the beryllium atom with two fewer electrons than silicon thus forming a (BeN_2O_2) tetrahedron isoelectronic with a (SiN_4) tetrahedron.[23] The substitution will probably reduce the bonding energy in part due to replacing of Be-O (1.624 Å) and SiO (1.623 Å) bonds (these are bond lengths in BeO and SiO_2) for Si-N bonds and partly due to stretching of the Be-O and Si-O bonds for accommodation in the Si_3N_4 lattice with average bond length of 1.736 Å. The reduced free energy of the solid solution brings about reduction of the energy for intrinsic defect formation (increased equilibrium defect concentration) and hence one expects enhanced self-diffusion. We believe that our experimental observations may be in support of the above model and that it may apply also to solid solutions in the system Si_3N_4-Al_2O_3-AlN.

The effect of metallic impurities on sintering observed in the present investigation requires substantially more quantitative measurements before a mechanism can be postulated. Nevertheless, one speculates that the impurities would be present during sintering as oxides or, more specifically, as silicate melts and solidify as an amorphous phase. This is indicated by the results of TEM. With a concentration of about 0.1% of Ca + Mg + Fe (see Table 12) a volume fraction of liquid about 1-2% could be easily formed (if enough oxygen was available). This volume of liquid is insufficient to bring about densification by the dissolution and reprecipitation mechanism. Indeed, such a composition will not densify on sintering. Yet impurities on such a level do promote densification to a certain extent under hot-pressing conditions. (A sample of Si_3N_4 with no additions yielded 82% density on hot-pressing under nominal conditions, while pure Si_3N_4 powders did not respond at all.) It is therefore possible that the sintering of Si_3N_4 under the experimental conditions of the present investigation proceeds by a combined effect of lattice and/or grain boundary diffusion coupled with liquid-assisted mass transport, similar to that of impure alumina or alumina with an addition of about 1% SiO_2 + MgO.

---

[23] P.E.D. Morgan, "Bonding in Nitrogen Ceramics" in Nitrogen Ceramics, F.L. Riley, ed., Noordhoff Leyden, 1977.

G. Summary of Sintering Results

a. $BeSiN_2$ is an efficient addition which promotes sintering of Si_3N_4 under specific conditions.

b. Additions of between 3.5 to 7% $BeSiN_2$, corresponding to 0.5 to 1% Be, brought about densification of four different Si_3N_4 powders to densities above 90%.

c. Powders derived from nitridation of silicon were milled to improve sinterability.

d. Densification is first observed near 1800°C (2% shrinkage) and terminates near 2100°C. Nitrogen pressures between 5 and 8.2 MPa were applied in successful sintering experiments.

e. Temperature in excess of 2100°C brought about bloating of some specimens.

f. At 2.75 MPa of nitrogen a substantial fraction of silicon formed in the specimen at 2080°C; at 1.35 MPa nitrogen a specimen totally decomposed.

g. Oxygen content > than 2% in the powders is necessary for sintering. Powders with lower oxygen levels sintered poorly.

h. Powders low in oxygen responded to sintering when 1.5% oxygen was introduced as SiO_2 or by exposure of the specimens to air at 900°C prior to sintering.

i. Carbon monoxide pressures up to 1.5 MPa do not interfere with sintering and, in some cases, promoted densification.

j. Even with control of the oxygen level substantial variation in degree of densification was observed. This variation has been linked to transport of minor amounts of Ca and Mg and perhaps Fe either into or out of the specimens during the early stages of sintering. These metallic impurities on a 500-1000 PPM level promote densification.

VIII. CHARACTERIZATION

A. Phase Composition

Phase composition and lattice parameters were determined by evaluation of X-ray Debye-Scherrer patterns. The technique had to be optimized to obtain the necessary resolution and to overcome current problems resulting from analyzing light elements. With some specimens diffuse patterns were obtained; the diffuseness of the diffraction lines could be traced to compositional gradients across the specimens or to compositional inhomogeneity which resulted in differences of lattice parameters. In some instances, when the core of the specimen and its periphery were analyzed separately these differences could be determined.

The dominating phase in sintered specimens has been always β-Si_3N_4 which showed, in most instances, decreased lattice parameters resulting from formation of solid solution of Be and oxygen as expected according to work of Huseby, et al.[24] In some specimens traces of other phases have been detected (BeO, $BeSiN_2$) and in addition some weak extraneous lines which could not be identified.

Some important observations have been summarized in Table 13. Experiment 1 and 2 done under hot-pressing conditions show that Si_3N_4 (containing 3.2% oxygen) reacts with $BeSiN_2$ at 1675°C and that BeO and probably Si_2N_2O appear as transient phases. After a 30 minute hold at this temperature, a β-Si_3N_4 solid solution has formed and no other crystalline phases are detected. Consequently, it is expected that at the onset of shrinkage (sintering) at 1800°C all $BeSiN_2$ reacted and a solid solution formed. However, in specimen no. 4 (Table 13) $BeSiN_2$ has been detected after sintering at 2080°C. Its presence may be understood by considering the difference in initial oxygen content of the starting powders and the following reaction sequence:

1. $BeSiN_2 + SiO_2 = BeO + Si_2N_2O$
2. $BeSiN_2 + Si_2N_2O = BeO + Si_3N_4$
3. $2BeSiN_2 + SiO_2 = 2BeO + Si_3N_4$
4. $XBeO + x/2\ SiO_2 + (1-x/2)\ Si_3N_4 \rightarrow Si_{3-x}\ Be_x\ N_{4-2x}\ O_{2x}$
5. $Si_2N_2O = SiO + Si + N_2$
6. $3Si_2N_2O = 3SiO + Si_3N_4 + N_2$

---

[24] I.C. Huseby, H.L. Lukas and G. Petzow, "Phase Equilibria in the System Si_3N_4-SiO_2-BeO-Be_3N_2," J. Am. Cer. Soc. 58, 377(1975).

TABLE 13. RESULTS OF X-RAY DIFFRACTION ANALYSES

Exp. No.	Specimen Composition	Starting Oxygen Content, wt%	Heat-treatment Density %	Lattice Parameters a	c	Other Phases Detected
1	SN-502-23A 7% $BeSiN_2$	3.2	Hot pressed at 1675°C-2 min, 75%	Diffuse lines, not measurable		BeO; Si_2N_2O
2	Same	3.2	Hot-pressed at 1675°C 30 min, 85%	7.590±.003	2.903±.001	None
3	Starck 118 + 3.5% $BeSiN_2$	1.8	Sintered at 2080°C, 94%	7.596±.003	2.904±.001	2 weak lines for d's 1.992 and 1.971 unidentified
4	In-House + 7% $BeSiN_2$	2.08	Sintered at 2080°C dense core >95%	7.590±.002	2.903±.001	Several unidentified weak lines for large d's $BeSiN_2$
	"	"	Porous periphery	7.598±.003	2.904±.001	Same; no $BeSiN_2$
5	Cerac B2 + 5% $BeSiN_2$	1.08	Sintered at 2100°C 73%	7.599±.001	2.9036±.0005	BeO
	Pure β-Si_3N_4 this work		2000°C	7.596±.001	2.904±.0005	None
	Impure β-Si_3N_4 Huseby(et al) (24)			7.6045	2.908	Not Given
	Impure β-Si_3N_4 Henderson and Taylor (26)			7.600±.001	2.908±.001	α-Si_3N_4, Si_2N_2O

$BeSiN_2$ reacts with SiO to yield BeO, Eq. 1, and BeO reacts further with additional SiO_2 and silicon nitride to form a solid solution (Eq. 4). If enough oxygen is available as SiO_2 both reaction 1 and 4 may go to completion. However, as these reactions compete for SiO_2 their relative reaction rate may control the fraction of $BeSiN_2$ reacted if less than the stoichiometric amount of oxygen is available. The stoichiometry necessary for completion of reaction 1 and 4 depends on whether Si_2N_2O reacts according to equation 2 or some oxygen is lost as SiO as shown by equations 5 and 6. If the former applied (i.e., the overall equation 3 followed by 4), then every mol of $BeSiN_2$ requires a mol of SiO_2 or in weight ratio, oxygen to $BeSiN_2$ is about 0.5. This has been the composition of experiment 1 and 2 (Table 13) and in agreement with predictions, no $BeSiN_2$ was found in the product. The composition of experiment 4 was however substoichiometric in the oxygen: $BeSiN_2$ ratio and, consequently, $BeSiN_2$ did not react to completion.

Si_2N_2O could, in part at least, decompose according to equations 5 and 6 which may further increase oxygen deficiency. This would be manifested by residual $BeSiN_2$ and under special circumstances possibly also by the appearance of free silicon. Small amounts of free silicon were frequently observed in sintered bodies by optical microscopy and may have been of this origin.

A separate investigation of reaction 1 has been undertaken. $BeSiN_2$ was mixed with SiO_2 and reacted under hot pressing conditions. Near 1500°C a rapid reaction occurred which resulted in formation of a low viscosity melt. The expected phases, BeO and Si_2N_2O, appeared with some delay and formed more rapidly as the temperature was increased. Thus in the first stage of chemical reaction in the present system a transient liquid is formed by the reaction of $BeSiN_2$ with SiO_2 which further reacts with Si_3N_4 directly or via BeO and Si_2N_2O to form the expected solid solution. It has been shown by hot-pressing experiments[25] that this transient liquid allows substantial densification between 1600-1700°C at which temperature it disappears within 30 min., being consumed by Si_3N_4.

The absence of shrinkage on sintering below 1800°C suggests that the transient liquid described above contributes little or not at all to densification in the absence of applied pressure; in other words, that the mechanisms of hot-pressing and sintering of this composition may be different.

---

[25] J.A. Palm and C.D. Greskovich, "Silicon Nitride for Airborne Turbine Application," Final Report General Electric SRD-78-076 (1978).

Another important result of the X-ray diffraction study has been the relation of lattice parameters to the initial oxygen content and final density. When the initial oxygen content was low (exp. No. 5, Table 13) the shrinkage of the unit cell is unobservable, i.e., very little Be and oxygen dissolved to form a solid solution, and also little shrinkage of the specimen occurred. The core of specimen in exp. 4, which sintered dense, shows a well measurable decrease of the a-lattice parameter (identical to exp. 2), indicating solid solution formation. A surface layer, about 1/2 mm thick around the dense core of this specimen was porous and showed no lattice contraction. The likely interpretation of this result is that during sintering, as a consequence of a very low P_{O2}, the solid solution started to decompose and the loss of oxygen from the surface layer inhibited its densification. This process then led to the typical nouniform shrinkage manifested by flaring of one end of the cylindrical specimen.

B. Microstructure

The characterization of microstructure and sub-microstructure in sintered Si_3N_4 samples was investigated to determine: (1) pore size, shape and distribution, (2) Si_3N_4 grain size, shape and distribution, and (3) the identification of secondary phases and their location and size. Optical microscopy, SEM, TEM and X-ray diffraction techniques, were employed to reveal the various microstructural features. It was very difficult to identify an active chemical etchant which permitted delineation of grain boundaries in polished sections. None of the hot mineral acids (HF, HNO_3, HCl, H_2SO_4) was effective. This was always the case when sintered material was prepared using Be_3N_2 or $BeSiN_2$ dopant along with highly-pure or impure Si_3N_4 powder. After considerable experimentation an excellent caustic etchant was identified, namely a melt of KOH, NaOH and LiOH (4:4:1 by weight, respectively) at about 180°C for 20 min. The use of this etchant combined with optical microscopy at high magnifications or, preferably, SEM permitted the observation of grain sizes and shapes in several of the fine-grained, sintered samples.

1. Porosity

The microstructures of three sintered samples of the same starting composition (Processed Starck Si_3N_4 + 3.5 wt% $BeSiN_2$) fired under the same thermal conditions (2030°C-15 min - 7.6 MPa of nitrogen pressure) except for using different packing powders in SiC tubes of different size are illustrated in Figure 12A, B, and C. Limiting densities were obtained for each of these three samples and only β-Si_3N_4 was detectable by standard X-ray diffraction methods. A typical microstructure of a low relative density (74%), sintered body of β-Si_3N_4 is shown in Figure 12A. It is characterized by an interconnected network of pores (black) and solid (grey) phase. Considerable growth of pores and grains has occurred because

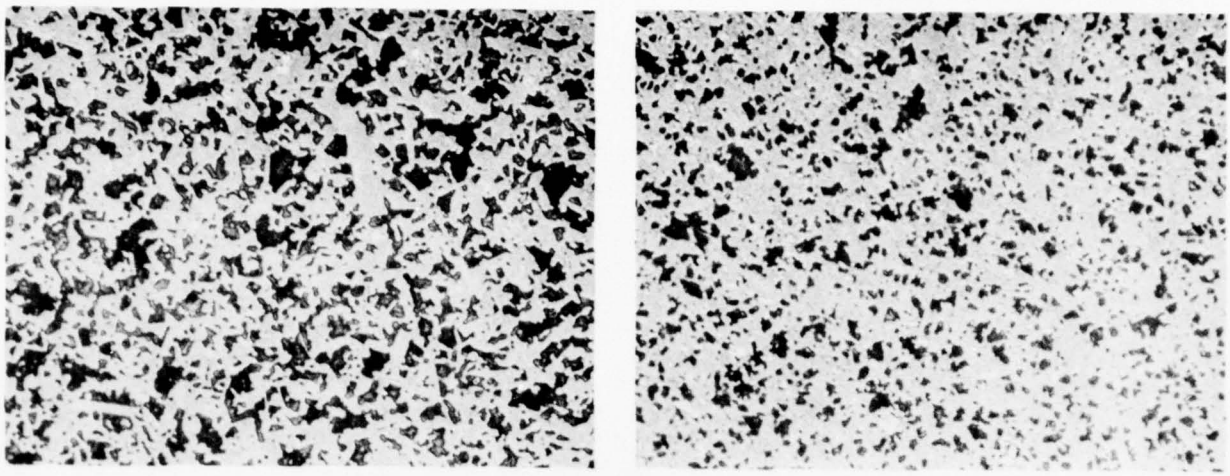

(A) (B)

(C)

Figure 12. Sintered Si_3N_4 of composition, Starck-possessed Si_3N_4 + 3.5% $BeSiN_2$, fired at 2030°C for 15 min. at 7.6 MPa of N_2. (A) Mixture of SiC/Si_3N_4 packing powder used in an 8 cm long SiC tube, relative density ≈ 74% Mag. = 500X. (B) Apache Si_3N_4 packing powder used in an 8 cm long SiC tube, relative density ≈ 84%, Mag. = 500X. (C) Reused SiC/Si_3N_4 packing powder in an 18 cm long SiC tube, relative density ≈ 98%, Mag. = 750X.

the average size of the pore and solid phases is 1-4 μ and 1-10 μ, respectively, as compared to ∿0.2 μ Si_3N_4 particles in the initial green compact of 55% relative density. Additional noteworthy features of the solid phase are the thin necks connecting larger solid-solid regions and the appearance of many straight-sided grains of high aspect ratio ≥ 5. This type of microstructure is characteristic of those found for other "unsinterable" covalent solids[22] such as Si and SiC. As the relative density of sintered Si_3N_4 is increased to ∿84%, the average pore size (Figure 12B) decreases and the number density of elongated (high aspect ratio) β-Si_3N_4 grains decrease. At this density light reflectivity from the solid phase is sufficiently high to distinguish bright particles of secondary phases scattered throughout the matrix. These bright particles have been identified as Si and SiC, both of which in part originate from the starting Si_3N_4 powder. The highest density achieved by sintering was 98% and the corresponding microstructure is shown in Figure 12C. The pore phase is discontinuous and achieves an average size ≤ 1.5 μ. The fine dispersion of the secondary phases of Si and SiC, about 2 μ or less in size, is more evident in this dense sample. This high density was achieved by: 1) using a longer SiC tube (18 versus 8 cm long) which is believed to suppress significant transport of C-bearing gaseous species to the Si_3N_4 compact, and 2) using a reused mixture of SiC/Si_3N_4 packing powder which becomes more impure with repetitive firings of impure Si_3N_4 compacts.

Similar sintering behavior is observed for compacts prepared from processed high purity Sylvania SN502 (S.A. ≈13m^2/g) Si_3N_4 powder mixed with 7 wt% $BeSiN_2$ (used as a sintering aid). A pore-grain structure (Figure 13A) similar to that shown in Figure 12A occurs for an 80% dense, sintered sample which was surrounded by a mixture of fresh and reused Apache packing powder. If, on the other hand, a reused mixture (20% Apache Si_3N_4 + 80% Lonza Sic) of packing powder surrounds the compact of the same initial composition, then sintered material with average relative densities near 94% may be prepared. The microstructure of such a sample presented in Figure 13B shows non-uniform pore distribution apparently due to non-uniform binder distribution in the green compact. The dense regions (Figure 13C) are over 98% density. It appears so far that the sintering behavior of the highly-pure Sylvania Si_3N_4 powder is sensitive to impurity effects.

The typical microstructure of a sintered compact, composed initially in Cerac Si_3N_4 powder + 7wt% $BeSiN_2$ + 3% SiO_2 and fired in a gaseous mixture of 8.5 atm CO + 53 atm N_2 at 2100°C is illustrated in Figure 14. The sample had a uniform microstructure but was only about 86% dense. This photomicrograph was particularly interesting because it shows that fine particles of β-SiC (bright reflecting phase) form in the β-Si_3N_4 matrix. This appears to be the general

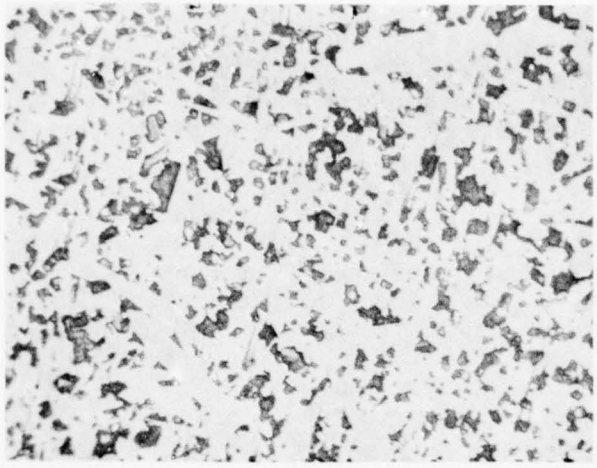

(A)

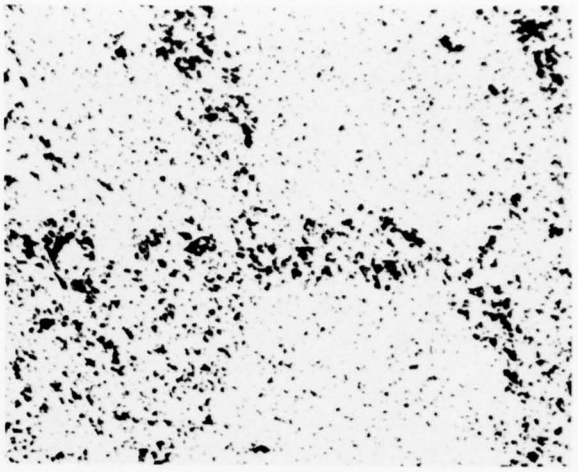

(B)

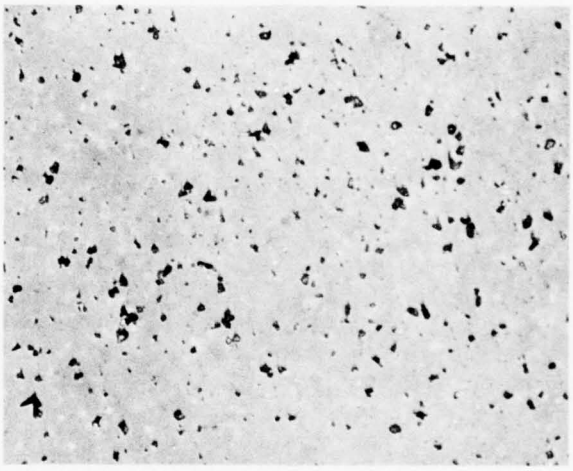

(C)

Figure 13. Reflected-light photomicrographs of microstructures of sintered Si_3N_4 (SN502-processed powder + 7 wt% $BeSiN_2$). (A) Powder compact surrounded with mixture of fresh and reused Apache packing powder, Mag. = 500X. (B) Packing powder was a reused mixture of 20% Apache Si_3N_4 and 80% Lonza SiC, Mag. = 200X. (C) Same as (B) except Mag. = 500X.

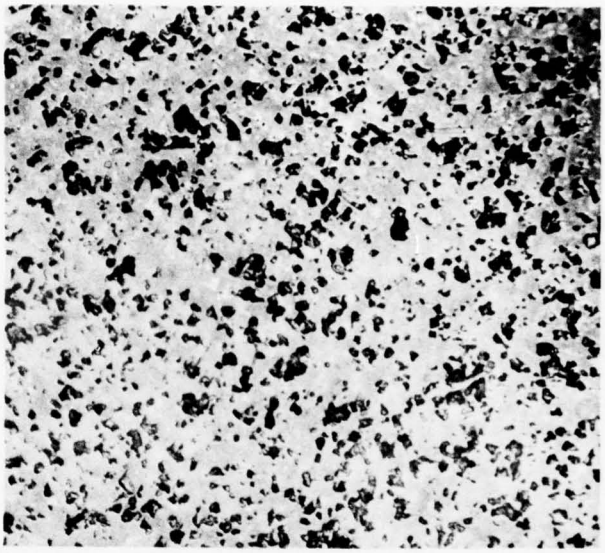

Figure 14. Photomicrograph showing SiC particles formed in Si_3N_4 during sintering in a CO/N_2 gaseous mixture at 2100°C.

case when substantial amounts of CO gas exists in the sintering atmosphere.

2. Density Gradients

Density gradients usually exist in compacts sintered to less than 95% relative density. The density of the surface region can be higher than that of the interior region. This observation is illustrated by Figures 15A and B and correlates with the presence of disconnected porosity in the surface region and a significant amount of interconnected porosity in the specimens' interior. Conversely, the specimen surface region can be more porous than the interior region (Figure 16). This phenomenon appears to be associated with gas/solid reactions and impurity effects in the vicinity of the sintering compact during firing. If impurities, such as Ca, are available in the prevailing atmosphere and diffuse into the compact, then the higher concentration of the impurity in the surface region will accelerate densification there and result in higher density in the surface region. An explanation offered for lower surface densities in sintered compacts is simply, but not conclusively, that too much oxygen, probably in the form of SiO, is lost from the β-Si_3N_4 solid solution during sintering, thereby decreasing the densification rate in the surface region. Density gradients also exist in sintered specimens that undergo visible bloating (Figure 17). Rapid heating rates ($\sim$200°C/min) and high sintering temperatures (>2100°C) usually give rise to bloating. Figure 17 shows a porosity gradient from

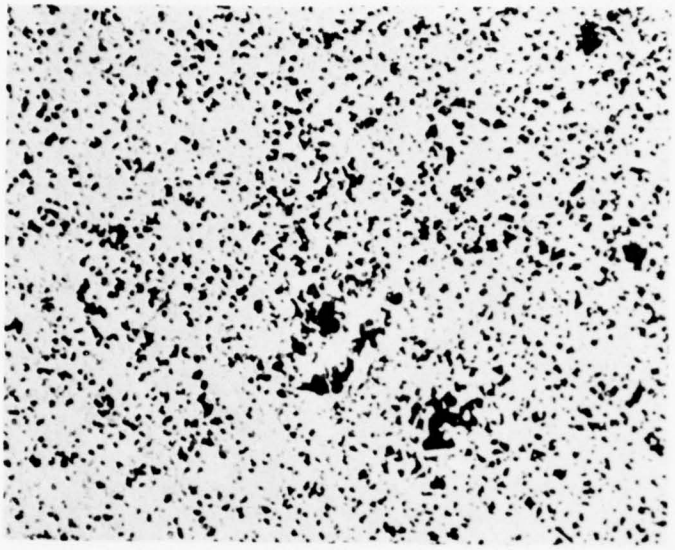

(A)

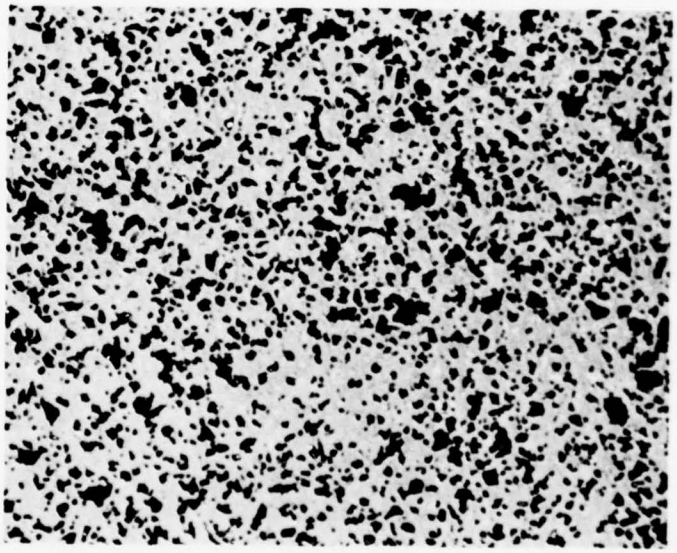

(B)

Figure 15. Sintered Si_3N_4 of composition Starck-processed Si_3N_4 + 3.5 wt% $BeSiN_2$, fired at 2030°C-15min-7MPa of N_2, relative density ≈88%. (A) Surface region. (B) Interior region. Mag. = 600X.

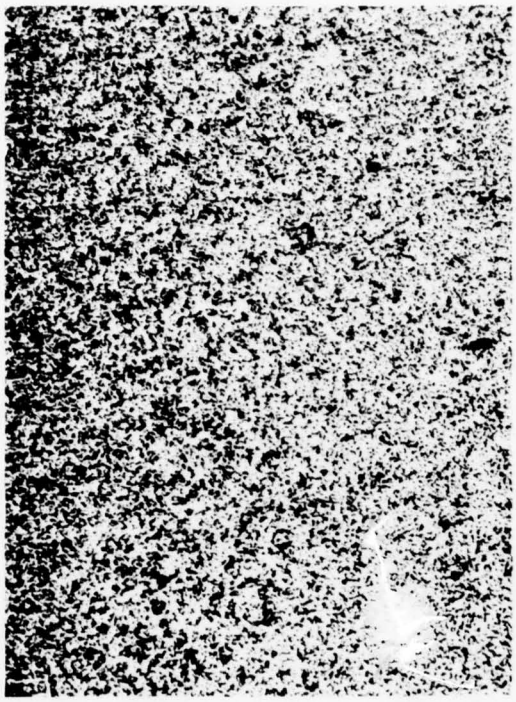

Figure 16. Typical density gradient observed in several sintered specimens, Mag. = 100X.

the specimen interior to the surface region. The large pores are frequently 30 μ in size or smaller and up to millimeter sized pores are found in the center of larger sintered specimens (∿1.3 x 0.5 cm). The gas evolution responsible for specimen bloating originates probably from thermal dissociation of the β-Si_3N_4 solid solution in regions of the specimen which are exposed to excessively high temperatures.

3. Grain Structure

A typical grain structure of a polished and chemically etched sintered specimen of composition high purity Si_3N_4 (93%) + 7 wt% $BeSiN_2$, having a relative density of 96%, is illustrated in Figure 18. Although the average grain size is estimated to be 2-3 μ, elongated β-Si_3N_4 grains up to 10 to 15 μ in length have grown in the matrix. An occasional bright particle of Si is also observed in the microstructure. In polarized light (Figure 19) many of the hexagonally-shaped grains appear dark or exhibit optical extinction. A high magnification picture of this same microstructure was taken by scanning electron microscopy (Figure 20A). Growth of elongated β-Si_3N_4 in a finer β-Si_3N_4 matrix is obvious. A number of hexagonal grains appear in the microstructure. In addition, there are a number of triangularly-shaped pores

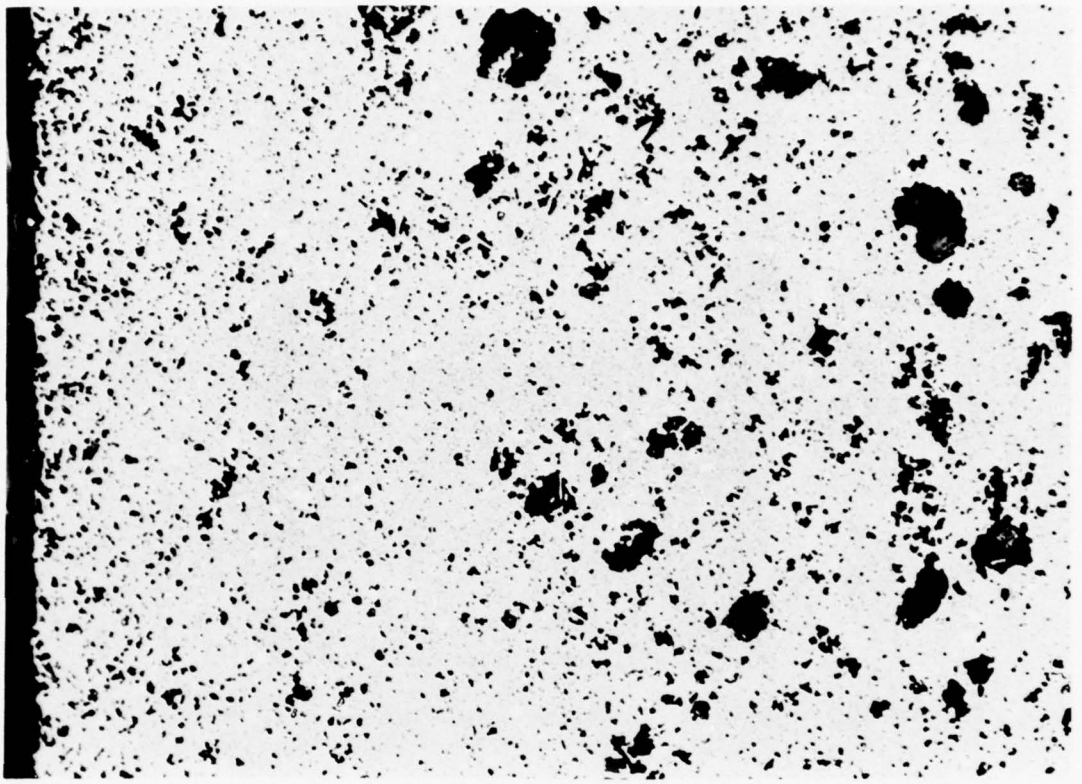

Figure 17. Typical microstructure of sintered Si_3N_4 that exhibited bloating. Fast heating rate ~200°C/min used to reach a soak temperature of 2080°C, Mag. = 300X.

at grain boundary triple points. These pores, as will be shown shortly, probably are a consequence of the dissolution (into the chemical etchant) of a wetting, grain boundary liquid phase. A very similar type of microstructure is also found for sintered Si_3N_4 made from Starck or Cerac powders along with $BeSiN_2$ as an additive (Figure 20B).

Transmission electron microscopy was used to elucidate the presence of a grain boundary phase in sintered Si_3N_4. Specimen preparation involved: (1) grinding a thin slice of the sample with 600 grit SiC to a thickness of 25 to 75 microns and (2) micromilling from both sides of the specimen with 6 KV Ar ions at an angle of 21° until a small hole formed in the center of the specimen and (3) examining the specimen in bright field transmission in a multi-tilt, Siemens Elmiskop 101 microscope at 125 KV. Approximately 100-200 grains were examined for a grain boundary phase in each sample. Only a few percent of the grain boundary intersections examined contained pockets of liquid phase (compositions containing 7 wt% $BeSiN_2$, Figure 21A and B. However,

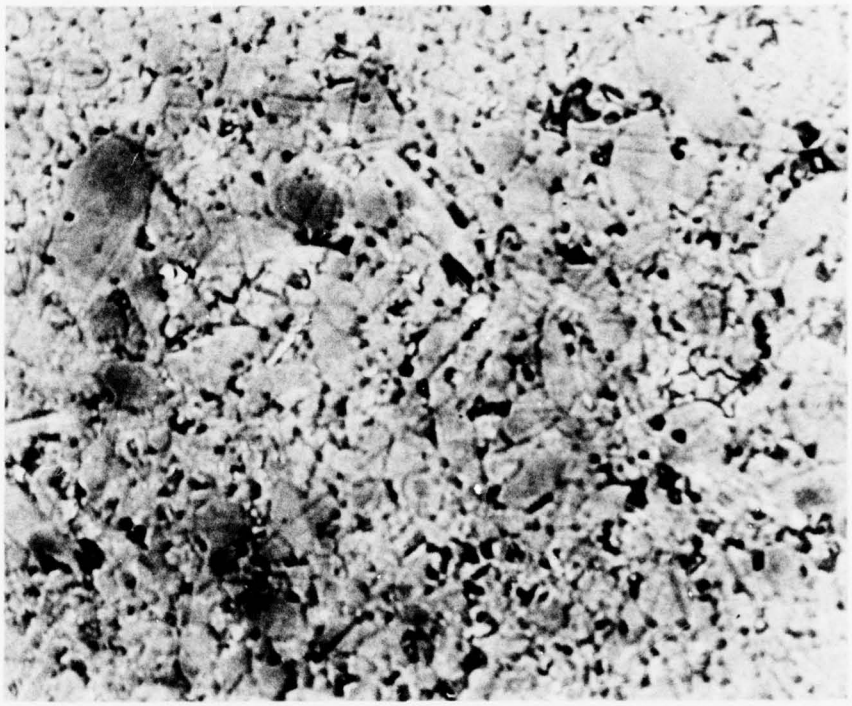

Figure 18. Grain structure in a polished and chemically-etched sample of sintered Si_3N_4 of composition, In-House Si_3N_4 + 7 wt% $BeSiN_2$. Sintered at 2050°C for 15 min in 8.4 MPa of N_2. Polished specimen chemically-etched in a hot mixture of NaOH, KOH and LiOH (4:4:1 parts, respectively) for 20 min at 180°C. Reflection Nomarski differential interference contrast, Mag. = 1500X.

for compositions containing both 1 wt% Be_3N_2 and 2% Mg_3N_2 (Figure 21C) pockets of liquid phase were observed on more than 5% of the grain boundary intersections. The triangular pocket of liquid phase between 3 β-Si_3N_4 grains shown in Figure 21A has the identical shape of the fine pores located at grain triple points in the SEM photomicrographs of Figure 20A. and B. Another small triangularly-shaped liquid pocket can be seen in Figure 21B, along with a much larger region of liquid phase surrounding a hexagonal, faceted β-Si_3N_4 grain about 1 μ in average dimension. Hexagonally-shaped, faceted β-Si_3N_4 grains generally are associated with neighboring liquid phase. This suggests that a quick method to determine the presence of a small amount of liquid phase in these ceramics is to use optical microscopy with polarized light which reveals the highly faceted, β-Si_3N_4 grains such as shown in Figure 19. The faceted interface of these grains may be related to anisotropy of solid/liquid surface energy with crystallographic orientation or to crystallization of the β-Si_3N_4 grains from the liquid phase.

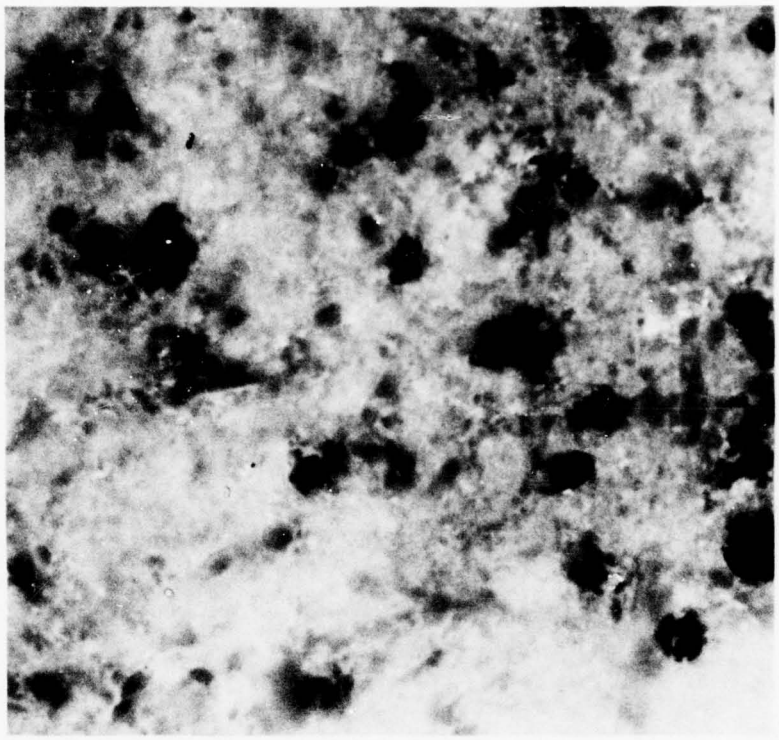

Figure 19. Different region of same specimen shown in Figure 17. Polarized light, Mag. = 1500X.

Finally, considerable effort was devoted towards applying TEM methods for detection of a continuous, amorphous (liquid) phase that completely wets the grain boundaries present in a few sintered samples. TEM photomicrographs of a number of grain boundaries at magnifications up to 200,000X using conventional tilting methods did not resolve a second phase film at grain-grain interface in sintered samples made with high purity In-House or Sylvania Si_3N_4 powder. The use of higher resolution lattice fringe techniques did reveal a very thin film, <10Å thick, between selected β-Si_3N_4 grains in $BeSiN_2$-doped sintered material made with high purity In-House Si_3N_4 powder (Figure 22A) and Sylvania SN502 powder (Figure 22B). Although many "clean" grain boundaries have been observed it is not possible to assert that a grain boundary phase is absent because of the difficulties in observation in the lattice imaging mode.

C. Creep

Creep was measured in three point bending at constant stress with specimens 0.25 x 0.25 x 3.0 cm on a 2.87 cm span. The jig of the creep rig is made of dense silicon carbide and consists of outer and inner tubes. The outer tube supports the specimen on two SiC pins; the inner tube transmits

(A)

(B)

Figure 20. Typical SEM photomicrographs of microstructural features observed in sintered material derived from (A) high purity Si_3N_4 powder and 7 wt% $BeSiN_2$ as a densification aid, Mag. = 4000X, and (B) Commercial Starck Si_3N_4 powder and 3.5 wt% $BeSiN_2$, Mag. = 7000X. White spots in (B) are surface contaminants.

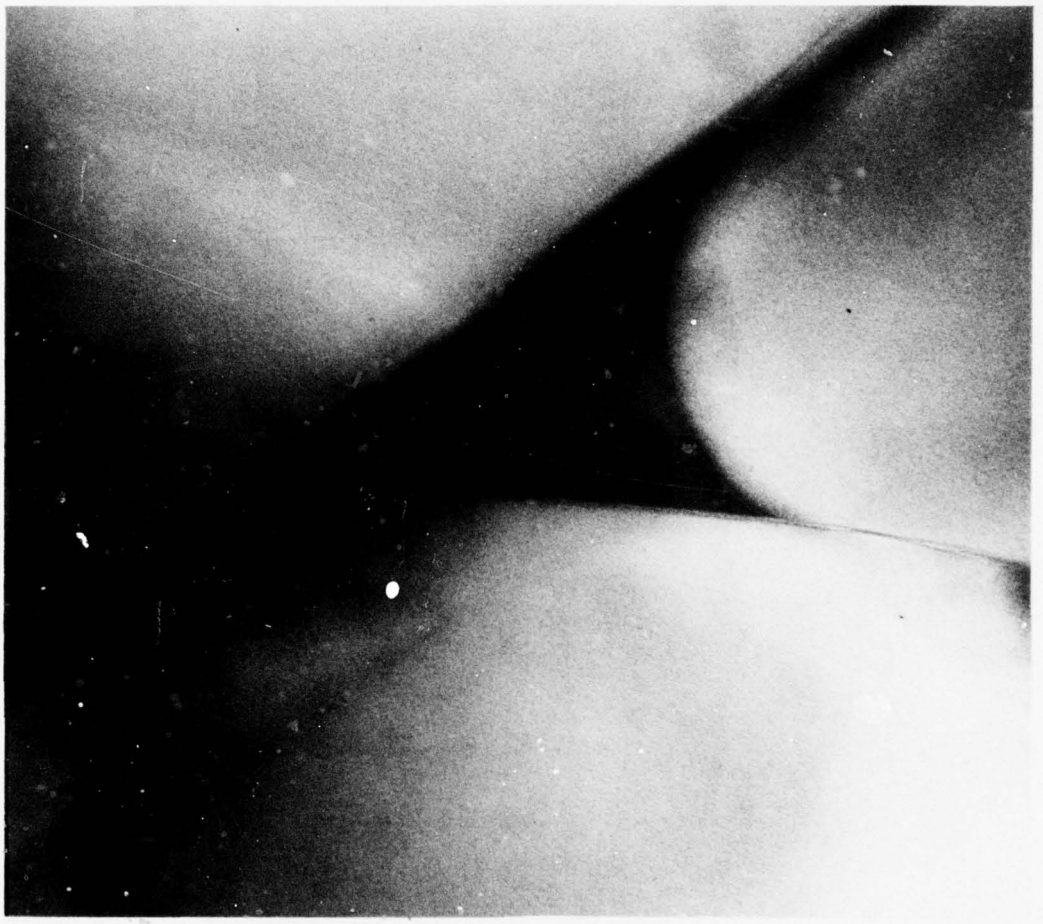

(A)

Figure 21. Electron transmission photographs of isolated pockets of liquid phase in sintered Si_3N_4 of composition (Si_3N_4-In-House + 7 wt% $BeSiN_2$), (A) Mag. = 150,000X and (B) Mag. = 100,000X. (C) Composition is Si_3N_4-In-House + 1% Be_3N_2 + 2% Mg_3N_2, Mag. = 175,000X.

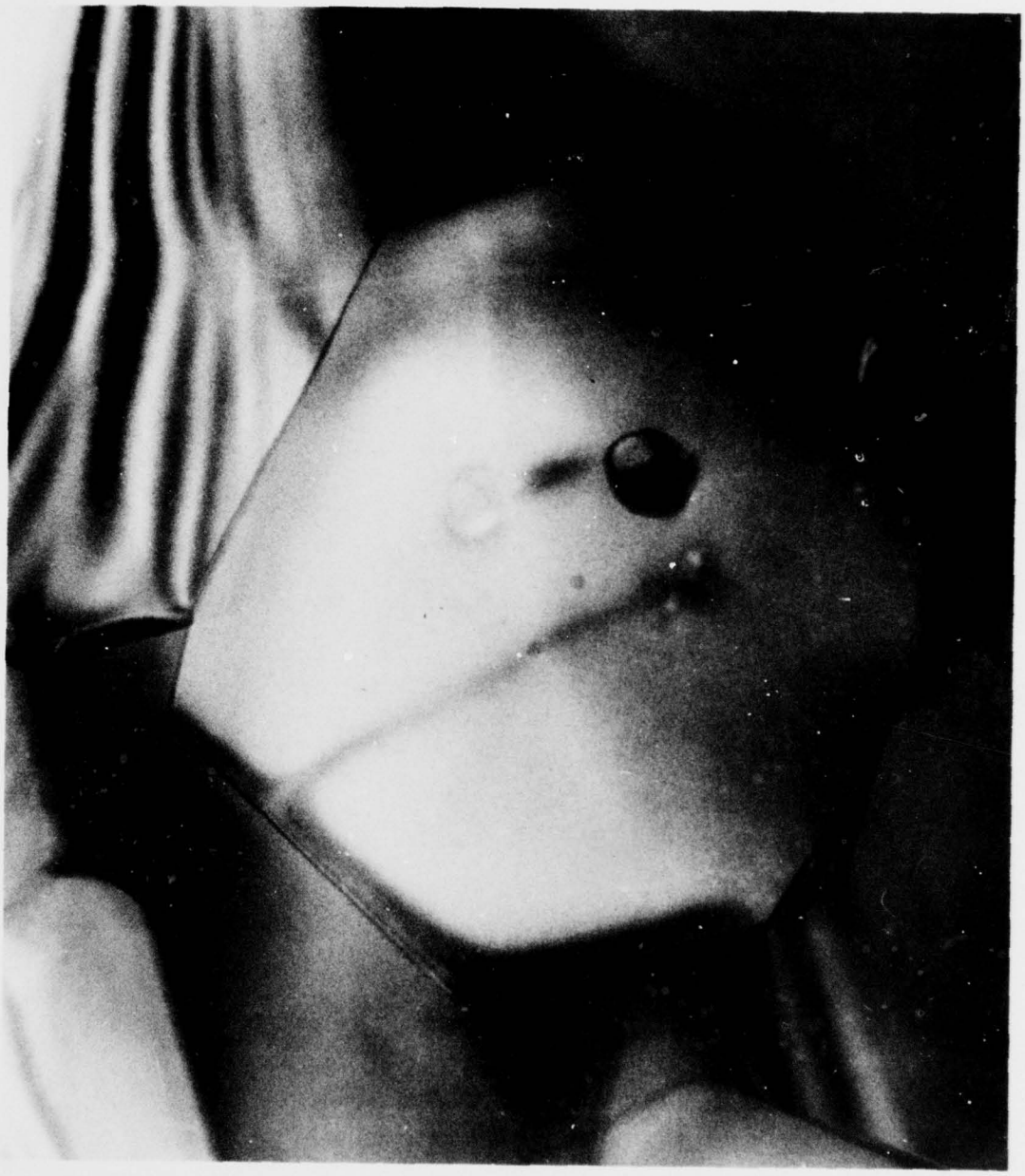

(B)

(C)

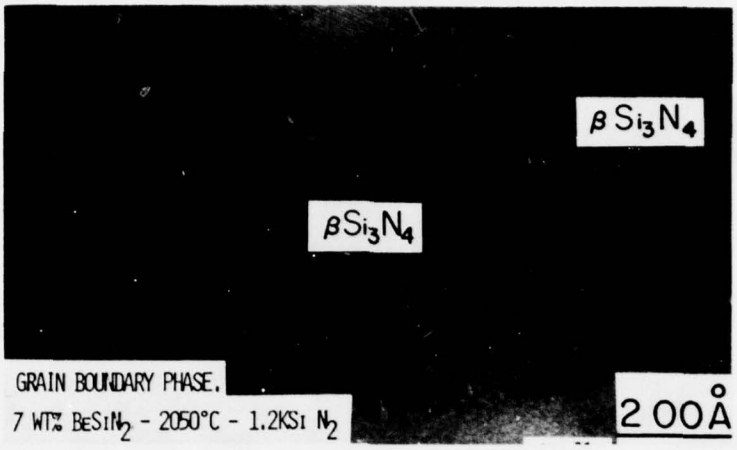

(A)

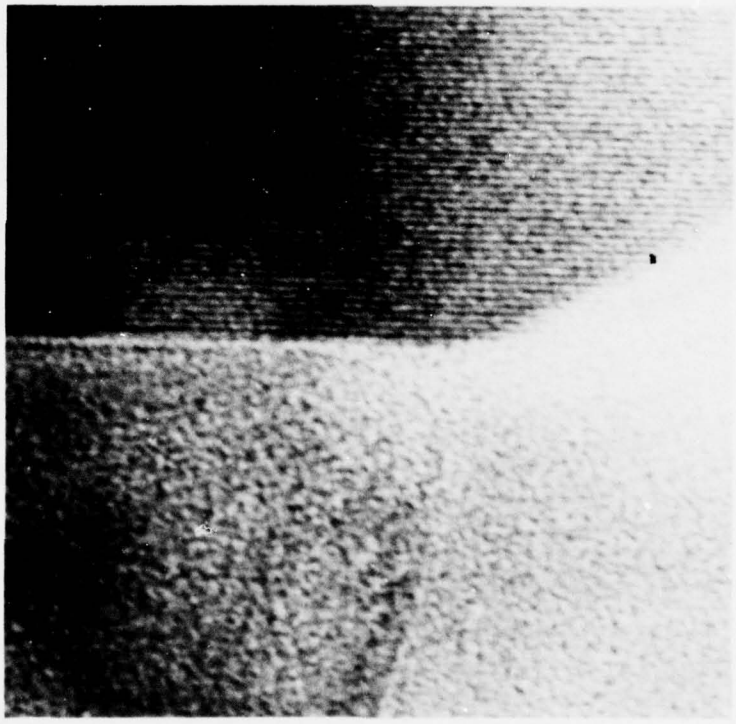

(B)

Figure 22. Lattice fringe photomicrographs of grain boundary region between neighboring grains of β-Si_3N_4 solid solution. Sintered samples were made from high purity starting powders, (A) In-House Si_3N_4 and (B) Sylvania SN502-Si_3N_4.

the deflection to an LVDT. The load is imposed by an independent system on the inner tube as shown schematically in in Figure 23. The system operates in air. The furnace is heated by molydisilicide heaters and is controlled by means of Pt/Rh thermocouples within about ±5°C. Previous experience has shown that the stiffness of the loading train was sufficient up to 1650°C. The difference in the deflection from the recorded trace and that determined by evaluation of the specimen's deformation after testing was 8%, which is considered good. Fluctuations of furnace and ambient temperatures along with some undetermined origin of noise limit creep measurements down to a strain rate of about 3×10^{-6}/hr and to an accuracy of ±10% at higher values of strain rate. Specimens were prepared by die pressing to shape, sintering in SiC tube furnace and machining to the desired dimensions. The deflection was obtained as a function of time by a recorded trace of the LVDT output through claibration (typically 4μ/1cm) and converted to outer fiber strain through the relation $\varepsilon = 6hy/L^2$, L=span and y=deflection. The strain rate was obtained from the slope of the tangent to the trace.

Data in Table 14 gives results obtained at 1450° with a specimen prepared from Si_3N_4 Starck sintered with 3.5% of $BeSiN_2$ at 2080°. Clearly the creep rate of this composition was decreasing over the whole testing period and the change of creep rate did not indicate that steady state creep would be obtained.

Transients are always observed in the initial period of a creep experiment due to several phenomena. With other materials, however, such as dense SiC or Al_2O_3, steady state

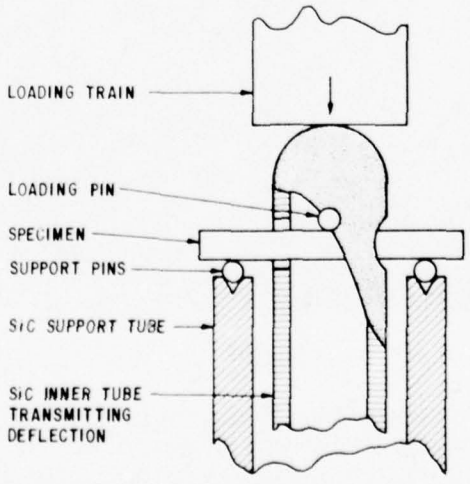

Figure 23. Schematic of specimen jig of the apparatus used in creep measurements.

TABLE 14. CREEP OF Si_3N_4 (STARCK 118) SINTERED WITH 3.5% $BeSiN_2$

Time Hrs.	Deflection μ	Creep Strain $\varepsilon \times 10^3$	Creep Rate $\varepsilon/hr \times 10^4$	Creep Rate $\dot{\varepsilon}/sec \times 10^7$	
1	3.87	0.7	6.6	1.83	Temp. 1450 ± 10°C
2	6.15	1.12	4.2	1.17	Outer fiber stress
4	9.65	1.76	3.3	0.92	26.2 MN/m^2
8	15.4	2.8	2.5	0.68	Spec. density 93.5%
16	23.5	4.3	1.67	0.46	Spec. dimensions
32	31.6	5.8	1.14	0.32	L 3.05 cm
48	37.3	6.8	0.75	0.21	W 0.255 cm
					span 2.87 cm
		CREEP OF SPECIMEN AFTER ANNEAL AT 1650°C-3 HRS			
1	3.03	0.57	5.0	1.39	Temp. 1450 ± 10°C
2	5.3	1.00	3.9	1.1	Outer fiber stress
4	9.46	1.77	2.8	0.78	24.6 MN/m^2
8	14.2	2.67	1.8	0.5	Spec. density 94.5%
16	19.5	3.7	1.0	0.28	Spec. dimensions
21	21.8	4.1	0.88	0.24	L 3.05 cm
					W 0.255 cm
					h 0.258 cm
					span 2.87 cm

creep is usually obtained with about ten hours at high temperature. It was suspected that the observed behavior could be related to a phase change, such as crystallization, proceeding at the temperature of the experiment. Such an effect is possible because of the rapid cooling rate used in the firing schedule for sintering. Therefore, another specimen was annealed at 1650°C for three hours and tested under identical conditions. The results (Table 14) were close enough to the first measurement, both in absolute values and trends, to discount an effect of annealing. The difference observed was attributed to the difference in specimen density.

Another specimen of the same composition was tested at 1300, 1350 and 1400°C. Creep rates obtained after 24 hours are in Table 15. This data does not appear to correspond to steady state creep because the problem of transient effects could not be resolved within the scope of this investigation. (The creep rate at 1450°, Table 15, was calculated from data in Table 14, for 24 hours and assuming a stress exponent of 1). It was possible to calculate an activation energy of 161 Kcal/mol but the involved uncertainty is large due to the difficulty of achieving constant creep rates.

A test bar 0.25 x 0.25 x 3.0 cm was machined for a specimen sintered from In-House, powder batch 20-21, with an addition

TABLE 15. CREEP RATE OF SINTERED "STARCK 118" Si_3N_4 + 3.5% $BeSiN_2$ at 69 MN/m^2

T°C	ε/hr	ε/sec
1300	0.25×10^{-5}	7×10^{-10}
1350	1.13×10^{-5}	3.14×10^{-9}
1400	5.7×10^{-5}	1.6×10^{-8}
1450	$3.3 \times 10^{-4*}$	$9.1 \times 10^{-8*}$

*Calculated from data in Table XVI using stress exponent 1.0 and 24 hours experiment time.

TABLE 16. CREEP OF IN-HOUSE Si_3N_4 SINTERED WITH 7% $BeSiN_2$, 1450°C

Stress (MN/m^2)	Time (Hr)	Strain(Cumulative) $\varepsilon \times 10^4$	Strain Rate $\varepsilon/hr \times 10^5$	$\varepsilon/sec \times 10^9$
41.4	24	0.93	1.55	4.3
82.7	24	1.5	2.7	7.4
138	24	2.8	4.5	12.5
212	7	3.7	13	36.6

of 7% $BeSiN_2$. The relative density of the bar was 90%. Results of a creep experiment made with this specimen at 1450°C are presented in Table 16. More extensive work was not warranted due to the relatively large residual porosity which could not be taken into account.

Fracture occurred after seven hrs. at 1450° at 212 MN/m^2 (30,000 psi) stress. Whether or not steady state creep was achieved in the selected time intervals was not established with certainty. The first three points in Table 16 (for stresses 41.4, 82.7 and 138 MN/m^2) yield a stress exponent near 1. However, the fourth point (for σ=212 MN) is substantially off the straight line, again indicating probably nonsteady creep.

The creep rate data obtained so far was plotted in Figure 24 and is compared with several measurements available in the literature on other Si_3N_4 ceramics. Also included is a set of data for hot-pressed material of the current composition, Si_3N_4-SN-502 + 7% $BeSiN_2$, obtained in this laboratory in a concurrent program.[25]

Ignoring an effect of porosity, the creep rate of the material prepared from the pure In-House powder is about a factor of 20 less than that of Starck Si_3N_4 measured at 1450° and 69 MN/m^2. However, such a comparison is superficial as it ignores grain size and does not reflect the actual potential of the two materials. Same applies, of

(25) J.A. Palm and C.D. Greskovich, "Silicon Nitride for Airborne Turbine Application," Final Report General Electric SRD-78-076 (1978).

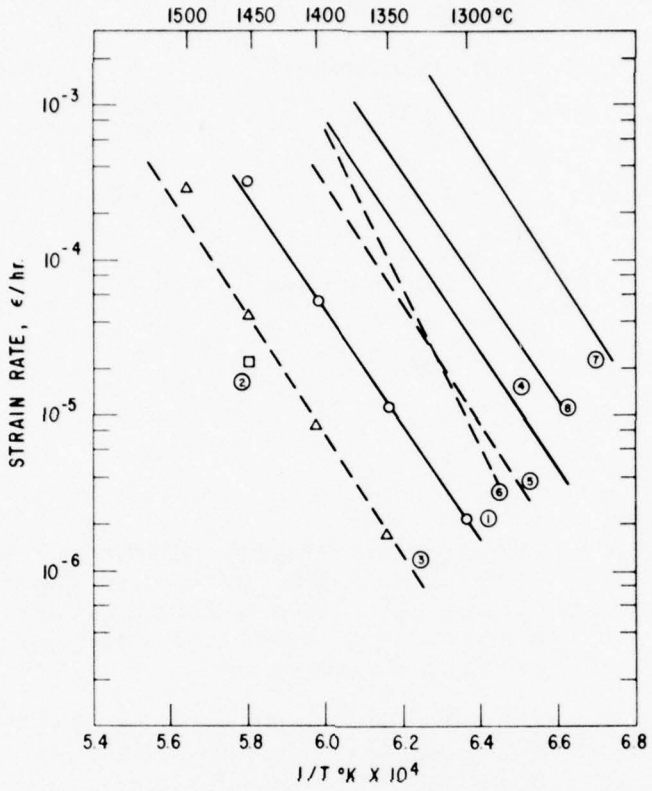

Figure 24. Creep rate of Si_3N_4 as a function of inverse temperatures, 1) Sintered Si_3N_4-Starck (this work), 2) Sintered pure In-House prepared Si_3N_4 (this work), 3) Hot-pressed Si_3N_4-SN-502 + 7% $BeSiN_2$ 3 pt. bending 69MN/m^2, (ref. 25). 4) HS-130, compression 69MN/m^2 Seltzer (ref. 26), 5) NC-132 compression 69 MN/m^2 Seltzer (ref. 26), 6) Si_3N_4 + 2.5% Ce_2O_3 hot-pressed 4 pt. bending 69 MN/m^2, Mazdiyasni (ref. 27), NC-132, tension at 17 MN/m^2, Kossowski, (ref. 28). 8) HS-130, 4 pt. bending, 60 MN/m2, Mazdiyasni (ref. 27).

---

(26) M.S. Seltzer, "High Temperature Creep of Silicon Base Compounds," Am. Cer. Soc. Bull. 56, 418(1977).

(27) K.S. Mazdiyasni and C.M. Cooke, "Consolidation Microstructure and Mechanical Properties of Si_3N_4 Doped with Rare-Earth Oxides," Jour. Am. Cer. Soc., 57, 536(1974).

(28) A.F. McLean, E.A. Fisher and R.J. Bratton, "Brittle Material Design," Report AMMRC-TR-73-32, January 1973.

course, for comparing the sintered and hot-pressed materials. It will be noticed from Figure 24 that creep rates of the sintered materials measured in this program are the lowest of any Si_3N_4 materials reported in the literature except NC 350 of Norton.

D. Oxidation Behavior of Sintered Si_3N_4

The oxidation behavior of various sintered compositions of Si_3N_4 (all containing some Be) was investigated at high temperatures (1400°C and 1550°C) in air by weight change measurements. During oxidation of Si_3N_4 there exists a net weight gain according to the reaction:

$$Si_3N_4 + 3O_2 \rightarrow SiO_2 + 2N_2 \uparrow$$

Singhal,[29] and Tripp and Graham[30] have shown that the oxidation of commercially-available, hot-pressed Si_3N_4 (Norton HS-130) exhibits parabolic behavior at temperatures up to 1500°C in air.

This is usually expressed by the parabolic rate equation,

$$(\Delta W/A)^2 = k_p t,$$

where $\Delta W/A$ is the change in weight per unit surface area, k_p is the parabolic rate constant and t is time. For Si_3N_4 this diffusion-controlled, oxidation behavior appears to be rate-limited by either oxygen or magnesium-impurity diffusion through the oxide scale composed of at least two phases, cristobalite and enstatite. Recently Cubicciotti, et.al.[31] presented oxidation data which suggests that the oxidation rate of NC-132 Si_3N_4, which is similar to that of HS-130 Si_3N_4, is controlled by diffusion of magnesium in the unoxidized Si_3N_4 material towards the substrate/oxide scale interface. The general results of these works show that the reaction rate during oxidation of Si_3N_4 depends primarily on the temperature, composition and microstructure of the oxide scale formed.

---

(29) S.C. Singhal, "Thermodynamics and Kinetics of Oxidation of Hot Pressed Si_3N_4," J. Mat. Sci., 11, 500-509(1976).

(30) W.C. Tripp and H.C. Graham, "Oxidation of Si_3N_4 in the Range 1300° to 1500°C," J. Am. Ceram. Soc., 59(9-10) 399-403(1976).

(31) D. Cubicciotti, K.H. Law and R.L. Jones, "The Rate Controlling Process in the Oxidation of Hot-Pressed Si_3N_4," J. Electrochem. Soc., Accelerated Brief Communications, 124, 1955-56 (1977).

Our oxidation experiments were carried out on cylindrical specimens cut from sintered pellets and having an apparent surface area of about 1.9 cm^2 and weight of ∿0.45g. Before oxidation these specimens were ground with 600 grit SiC to remove any surface deposits, cleaned with concentrated HF, and HCl rinsed with distilled water and dried. In spite of expected surface roughness the measured surface area was that for a smooth surface.

Oxidation of test pieces of sintered Si_3N_4 was performed in an Al_2O_3 tube furnace in air. New Al_2O_3 tubes (≈55 cm x 2.5 cm) were first baked-out at 1700°C for 24 h to volatilize alkali impurities which may have spurious effects on the oxidation rate of Si_3N_4. The Si_3N_4 specimen was placed on a SiC setter which lay on an Al_2O_3 boat. This assembly was inserted within 2 minutes into the hot furnace maintained at the desired oxidation temperature. In all cases the oxidation atmosphere was air flowing at ∿5cc/sec. Specimens were periodically removed from the furnace and their weight measured on a Mettler H54 AR balance capable of measuring weight reproducibly to the nearest 2 x 10^{-5}g. The square of the weight gain/unit area divided by oxidation time is a measure of the oxidation rate since the oxidation kinetics approximated nearly parabolic behavior.

The oxidation rates at 1405°C of three sintered compositions are shown by the parabolic plots in Figure 25. The three forms of sintered Si_3N_4 were prepared from: 1) Sylvania SN502 processed Si_3N_4 powder +7wt% $BeSiN_2$, 2) Cerac processed Si_3N_4 powder + 7 wt% $BeSiN_2$ + 3 wt% SiO_2 and 3) Starck processed Si_3N_4 powder + 3.5 wt% $BeSiN_2$. The sintered samples all had about the same relative density, ≈94%, and were oxidized simultaneously in the same furnace. It is apparent from the oxidation data at 1405°C in air that the oxidation rate constant (k_p) increases in going from Sylvania (k_p = 2 x 10^{-11} kg^2 m^{-4} s^{-1}) → Cerac (k_p = 7 x 10^{-11} kg^2 m^{-4} s^{-1}) → Starck (k_p = 15 x 10^{-11} kg^2 m^{-4} s^{-1}) sintered Si_3N_4. Although the nominal compositions are different and might, in part, be responsible for the trend, it is interesting to point out that the purity of the starting Si_3N_4 powders (see Table 1) decreases in going from Sylvania → Cerac → Starck. As a reference for comparison, however, our sintered Si_3N_4 compositions, containing $BeSiN_2$ additive, have far improved oxidation resistance than Norton's hot-pressed NC-132 Si_3N_4, containing ∿1 wt% MgO as a densification additive. Figure 25 shows that the oxidation rate of NC-132 Si_3N_4 exhibits parabolic behavior during about the first 30 hours of oxidation, but for longer times the rate of oxidation decreases with time at temperature. In the parabolic region the calculated oxidation rate constant (k_p) for hot pressed NC-132 Si_3N_4 is 66 x 10^{-11} kg^2 m^{-4} s^{-1} which is about a factor of 33 higher than our sintered material prepared from high-purity Sylvania Si_3N_4 powder. The improvement in oxidation resistance of any of the sintered compositions over that of Norton's NC-132

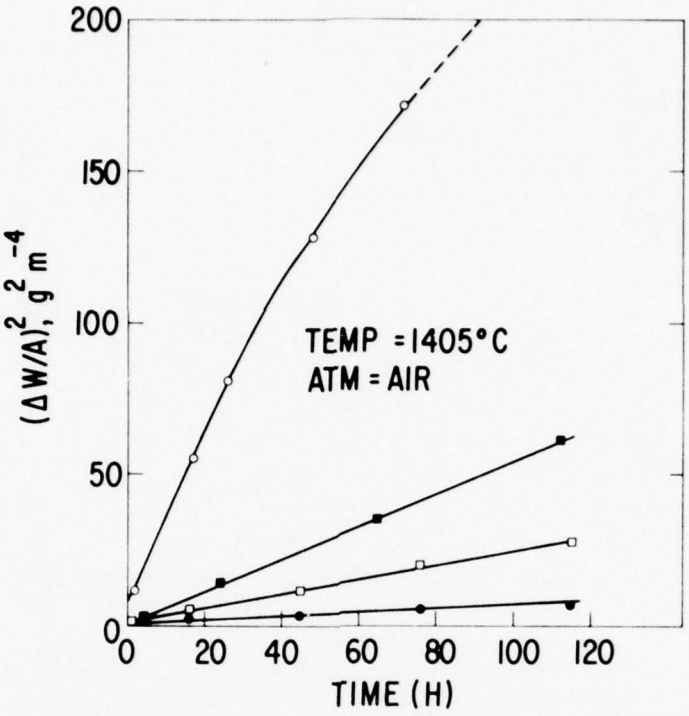

Figure 25. Oxidation kinetics of sintered Si_3N_4 compared to Norton's NC-132 hot-pressed Si_3N_4 at 1405°C in air. All specimens ≈94% dense. (●) Sylvania SN-502-processed powder used, (□) Cerac processed powder, (■) Starck processed powder and (O) Norton NC-132 hot-pressed Si_3N_4.

Si_3N_4 is directly related to the use of small amounts of $BeSiN_2$ instead of MgO as a densification aid.

The oxidation results at 1550°C in air for several compositions of sintered Si_3N_4 containing $BeSiN_2$ is shown in Figure 26. The oxidation data of nearly theoretically-dense, hot-pressed Si_3N_4 containing 2 wt% Be_3N_2 are used for comparison because the desired reference material, NC-132 Si_3N_4, exhibits catastropic oxidation at 1550°C. For those cases where several data points exist for each material, the data approximate a straight line, indicating parabolic oxidation kinetics. The oxidation rate of a 92% dense, sintered Si_3N_4 prepared from Starck-processed Si_3N_4 powder with a 3.5 wt% $BeSiN_2$ additive was surprisingly low and almost identical to nearly fully dense, hot pressed Si_3N_4. For example, the weight gain of this sintered sample was ≈3 g/m^2 after an oxidation exposure time of 18 h at 1550°C in air. This corresponds to a parabolic rate constant of about 13×10^{-11} $kg^2\ m^{-4}\ sec^{-1}$ and is comparable to the oxidation rate found for sintered material of the same nominal composition oxidized at 1405°C. This unusual observation is best explained by the

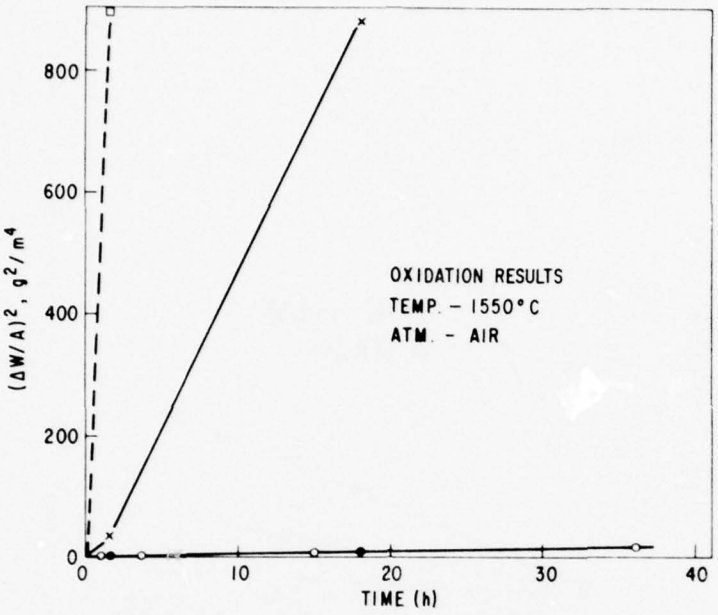

Figure 26. Oxidation results of selected compositions of sintered Si_3N_4 at 1550°C in air. (□) In-House Si_3N_4 + 7 wt% $BeSiN_2$, 93% relative density; (●) Starck-processed Si_3N_4 + 3.5 wt% $BeSiN_2$, 92% dense; (X) Starck-processed Si_3N_4 powder + 3.5 wt% $BeSiN_2$ + 1 wt% AlN, 92% dense; (O) high density (99%), hot pressed Si_3N_4 (In-House Si_3N_4 powder + 2 wt% Be_3N_2).

fact that the two green compacts were sintered in packing powders of different chemistry such that a higher purity packing powder was used to surround the sintered sample subsequently oxided at 1550°C. This would suggest, then, that impurities such as Ca, Mg, Fe and Al may be transported from the Si_3N_4 packing powder to the powder compact during high temperature sintering. An alternative explanation may be that there is more weight loss due to vaporization of SiO_2 at 1550°C than at 1405°C, resulting in apparently smaller weight gains than expected at 1550°C.

The addition of 1 wt% AlN to the Starck Si_3N_4 powder containing 3.5 wt% $BeSiN_2$ results in sintered samples with a dramatic increase in oxidation rate, as shown in Figure 26. The single point oxidation behavior of 92% dense, sintered Si_3N_4 prepared from high purity (In-House) Si_3N_4 powder plus 7 wt% $BeSiN_2$ is also included in Figure 26. The unexpectedly high weight gain/unit area measured was probably due to the presence of some open porosity, detectable by water absorption during density measurement, and to appreciable impurity pick-up from the impure packing powder used during sintering.

Characterization of the oxide scales was followed by X-ray diffraction, scanning electron microscopy and optical microscopy. The character of the oxide scale after 115 h at 1405°C on sintered material prepared from Sylvania powder is illustrated in Figure 27A. The oxide layer at the oxide/air interface is characterized by a network of fine microcracks or "mud-flat" cracks characteristic of the $\beta \rightarrow \alpha$ cristobalite transformation on cooling and a trace amount of a needle-like second phase. X-ray diffraction analysis shows only α-cristobalite present in the oxide scale. This oxide film is very coherent, thin and slightly "glassy" in appearance with no obvious evidence of large bubble or pore formation. Figure 27B shows the oxidized surface of sintered "Cerac" Si_3N_4 after 115 h of exposure to air at 1405°C. Microcracking of the oxide scale is also evident but featherlike, presumably β-cristobalite regions form at temperature. X-ray diffraction shows only α-cristobalite along with a few, weak unidentified peaks. Ths use of SEM equipped with a solid state X-ray detector revealed that the featherlike regions as well as the "matrix" oxide scale are composed primarily of Si, probably SiO_2, with the detection of Ca, Mg and Al. These latter impurities originate: 1) from diffusion from the unoxidized Si_3N_4 to the oxide/air interface, as previously reported during oxidation of hot pressed Si_3N_4, or 2) from impurity transport from the Al_2O_3 tube to the specimen surfaces during prolonged oxidation. X-ray diffraction analysis of oxidized "Starck" Si_3N_4 showed the appearance of a trace amount of Be_2SiO_4, phenacite, in addition to the major phase of α-cristobalite. The lack of detection of Be_2SiO_4 or BeO in oxide scales in sintered "Sylvania and Cerac" samples is possibly due to the thinner oxide layers formed in these higher-purity, sintered samples.

The oxide scales formed on sintered specimens at 1550°C were also visibly coherent and smooth for $(\Delta W/A)^2$-values less than $50 g^2 m^{-4}$. An occasional region of nonuniform oxidation observed contained small gas bubbles (probably N_2 filled) and was probably related to improper processing or contamination from furnace impurities. Those specimens which exhibited $(\Delta W/A)^2$-values greater than $800 g^2 m^{-4}$ had rough oxide coatings that contained gas bubbles and partially spalled-off. X-ray diffraction analyses showed that the oxidized layer on all sintered compositions investigated was composed of α-cristobalite and a trace amount of Be_2SiO_4 or possibly BeO.

E. Indentation Hardness

A selection of Si_3N_4 specimens was ground and polished and tested for microhardness by a Knoop indenter at a 500 g load. The data summarized in Table 17 are averages of six readings and indicate that residual porosity controls microhardness. The small variation in the chemical composition of the specimens would not be expected to reflect itself substantially. We note that these data do not necessarily

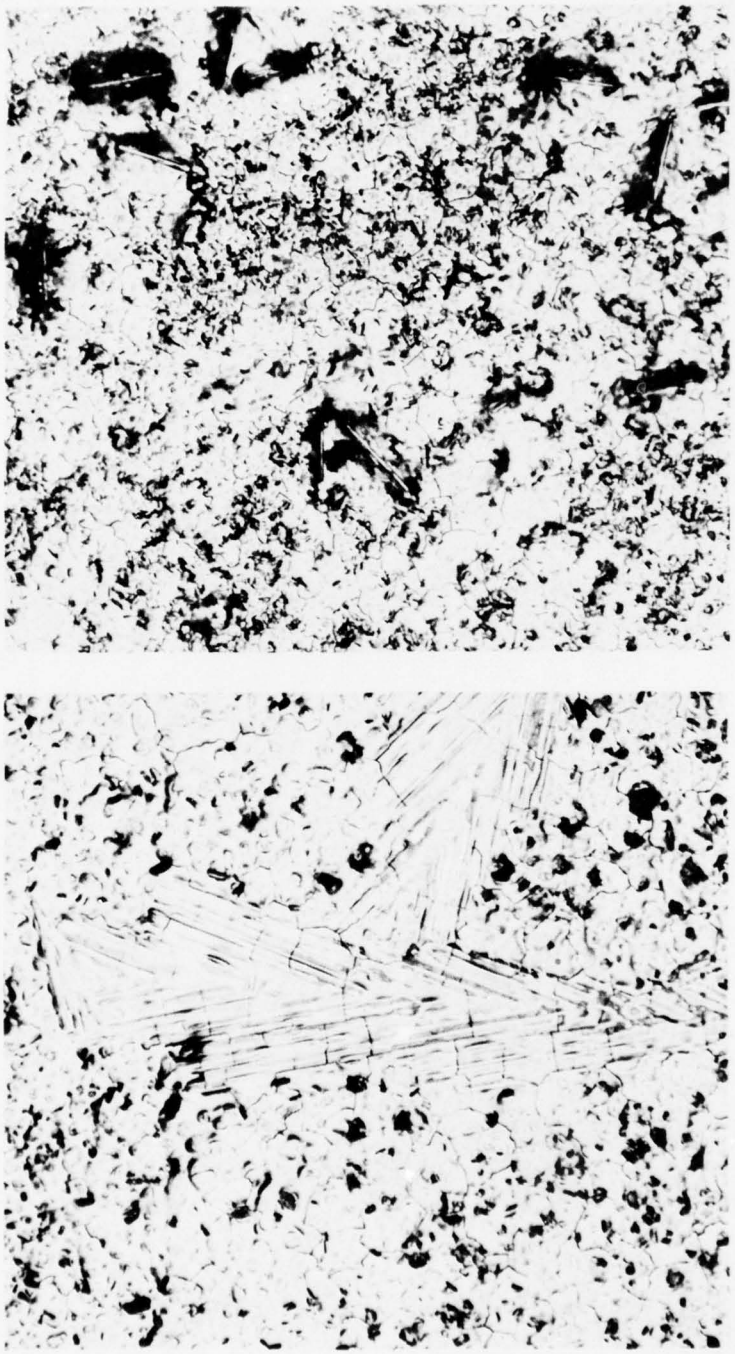

(A)

(B)

Figure 27. Typical photomicrographs of oxide scale at oxide/air interface after 115 h. of oxidation at 1405°C. (A) Sintered Si_3N_4 (Sylvania SN-502-processed + 7 wt% $BeSiN_2$ and (B) Sintered Si_3N_4 (Cerac-processed + 7 wt% $BeSiN_2$) Mag. = 300X.

TABLE 17. INDENTATION HARDNESS, KNOOP - 500g LOAD

Powder and Specimen Code	Relative Density%	Knoop Hardness No.
In-House Hot pressed	99+	1800
In-House Sinterd No 12c	96	1410
SN-503-23A Hot pressed, 3-SN-31	100	1820
SN-503-23A Sintered No. 140	96.5	1490
Starck-118 Sintered No. 94	94.5	1390
Cerac B2 Sintered No. 159	98.3	1720

represent hardness of silicon nitride but refer to a solid solution of an approximate composition $Si_{2.9}Be_{0.1}N_{3.8}O_{0.2}$.

F. Thermal Expansion

Thermal expansion was measured on one specimen prepared from Si_3N_4 powder Starck - batch 118, sintered to 93% with addition of 3.5% $BeSiN_2$, and one from In-House powder sintered with 7% $BeSiN_2$ to 91%. Both specimens were rods 35 mm long 3.5 x 3.5 mm. The measurement was carried out in a fused-quartz dilatometer in air up to 1000°C. The results presented in Table 18 compare well to $\alpha \approx 3.29 \times 10^{-6}/^{\circ}C$ measured by X-ray data for β-Si_3N_4 by Henderson and Taylor.[32] The difference between the two measurements, about 4%, is believed real and may be related to compositional differences.

G. Fracture Modes of Sintered Si_3N_4

The fracture behavior of sintered Si_3N_4 ceramics with relative density greater than 96% is illustrated in Figure 28A, B, and C. The sintered specimens are derived from different starting Si_3N_4 powders, contain 7wt% $BeSiN_2$ (In-House and Cerac Si_3N_4 powder) or 3.5 wt% $BeSiN_2$ (Starck), and have an average grain size between about 2 and 3 μ. A TEM replica of a fractured surface shown in Figure 28A shows

TABLE 18. RESULTS OF THERMAL EXPANSION MEASUREMENTS HIGH-PURITY IN-HOUSE Si_3N_4 + 7% $BeSiN_2$

T°C	Expansion	α/°C 25-T
200	0.032	1.83×10^{-6}
400	0.092	2.45×10^{-6}
600	0.164	2.85×10^{-6}
800	0.250	3.22×10^{-6}
1000	0.345	3.54×10^{-6}
	STARCK, 118 + 3.5% $BeSiN_2$	
200	0.030	1.71×10^{-6}
400	0.086	2.29×10^{-6}
600	0.155	2.69×10^{-6}
800	0.235	3.03×10^{-6}
1000	0.329	3.37×10^{-6}

the fracture occurred via a mixed mode process. Both intergranular and transgranular fracture processes are evident by the appearance of polyhedral faces on many grains and the large, smooth and sometimes rippled regions, respectively. Similarly, scanning electron micrographs presented in Figure 28B and C also illustrate the dual fracture mode and the typically "rough" fracture surface characteristic of most Si_3N_4 ceramics.

(A)

Figure 28. Mixed fracture modes observed in sintered Si_3N_4 of three compositions. (A) TEM replica of fractured surface of sintered Si_3N_4 (processed Sylvania Si_3N_4 + 7 wt% $BeSiN_2$), Mag. = 12,500X. (B) SEM of fractured surface of sintered Si_3N_4 (processed Cerac Si_3N_4 + 7 wt% $BeSiN_2$), Mag. = 3,000X. (C) SEM of fractured surface of sintered Si_3N_4 (Processed Starck Si_3N_4 + 3.5 wt% $BeSiN_2$), Mag. = 5,000X.

(B)

(C)

REFERENCES

1. C.D. Greskovich, S. Prochazka and J.H. Rosolowski, "Basic Research on Technology Development for Sintered Ceramics," November 1976, Final Report AFML-TR-76-179.

2. G.R. Terwilliger and F.F. Lange, "Pressureless Sintering of Si_3N_4" J. Mat. Sci., 10, 1169(1975.

3. D.J. Rowcliffe and P.J. Jorgensen "Sintering of Silicon Nitride," Proceedings of the Workshop in Ceramics for Advanced Heat Engines, January 1977, F.C. Moore, ed.

4. S.T. Buljan and R.N. Kleiner, "Cold Pressed and Sintered Si_3N_4" Annual Meeting of Am. Cer. Soc., Cincinnati, 1976.

5. J.T. Smith, "Properties of Fully Dense Sintered Si_3N_4 Composition," Fall Meeting of the Basic Science Group of the Am. Soc., Hyannis, Massachusetts, 1977.

6. H.F. Priest, G.L. Priest and G.E. Gazza, "Sintering of Si_3N_4 under N_2 Pressure," J. Am. Ceram. Soc., 60, 81(1977).

7. M. Mitomo, "Pressure Sintering of Si_3N_4" J. Mat. Sci. 11, 1103(1976).

8. M. Mitomo, M. Tsutsumi, E. Bannai and T. Tanaka, "Sintering of Si_3N_4" Am. Cer. Soc. Bull. 55, 313(1976).

9. I. Oda M. Kaneno and N. Yamamoto, "Pressureless Sintered Si_3N_4" in Nitrogen Ceramics, F.L. Riley, ed., Noordhoff Layden, 1977.

10. N. Clausen and J. Jahn, "Mechanical Properties of Sintered and Hot Pressed Si_3N_4-ZrO_2 Composites," J. Am. Cer. Soc. 61, 94(1978).

11. K. Komeya, et al., "Silicon Nitride Ceramics for Gas Turbine Engines," Paper No. 65, Proceeding of the Tokyo Joint Gas Turbine Congress, Tokyo, 1977.

12. K.H. Jack and W.J. Wilson, Nature 283, 28(1972).

13. JANAF Thermochemical Tables, U.S. Government Printing Office, Washington, D.C., 1971.

14. P.D. St. Pierre and M.J. Curran, "A Simple Laboratory Furnace for Temperatures Up to 2500°C," General Electric Report No. CRD-012, December 1972.

15. J. Drowart and G. DeMaria, "Thermodynamic Study of the Binary System Carbon-Silicon Using a Mass Spectrometer" in Silicon Carbide, J.R. O'Connor and J. Smiltens, eds., Pergamon Press, New York, 1960.

16. S. Wild, D. Grieveson and K.H. Jack, "The Thermodynamics and Kinetics of Formation of Phases in the Ge-N-O and Si-N-O Systems," Special Ceramic, No. 5, Brit. Cer. Res. Assoc., Stroke-On-Trent, June 1972.

17. H.G. Maguire and P.D. Augustus, "The Detection of Silicon-Oxynitride Layers on the Surfaces of Silicon-Nitride Film by Auger Electron Emission," J. Electrochem. Soc., 791-93, June 1972.

18. T.R. Wright and D.E. Niesz, "Improved Toughness of Refractory Compounds," NASA Report No. CR-134690(1974).

19. C.D. Greskovich, J.H. Rosolowski and S. Prochazka, "Ceramic Sintering," Final Report, 1975, General Electric SRD-75-084.

20. P. Eckerline, A. Rabenau and H. Nortmann, "Darstellung and Eigenschaften on $BeSiN_2$," Z. An u. Alg. Chem. 353, 113(1967).

21. J. DAvid and J. Lang, "Sur un nitrure de magnesium et de silicium," C.R. Acad. Sci. 261, 1005(1965).

22. C.D. Greskovich and J.H. Rosolowski, "Sintering Covalent Solids," J. Am. Cer. Soc., 59, 336(1976).

23. P.E.D. Morgan, "Bonding in Nitrogen Ceramics" in Nitrogen Ceramics, F.L. Riley, ed., Noordhoff Leyden, 1977.

24. I.C. Huseby, H.L. Lukas and G. Petzow, "Phase Equilibria in the System Si_3N_4-SiO_2-BeO-Be_3N_2," J. Am. Cer. Soc. 58, 377 (1975).

25. J.A. Palm and C.D. Greskovich, "Silicon Nitride for Airborne Turbine Application," Final Report General Electric SRD-78-076, (1978).

26. M.S. Seltzer, "High Temperature Creep of Silicon Base Compounds," Am. Cer. Soc. Bull. 56, 418(1977).

27. K.S. Mazdiyasni and C.M. Cooke, "Consolidation Microstructure and Mechanical Properties of Si_3N_4 Doped with Rare-Earth Oxides," Jour. Am. Cer. Soc., 57, 536(1974).

28. A.F. McLean, E.A. Fisher and R.J. Bratton, "Brittle Material Design," Report AMMRC-TR-73-32, January 1973.

29. S.C. Singhal, "Thermodynamics and Kinetics of Oxidation of Hot Pressed Si_3N_4," J. Mat. Sci., 11, 500-509(1976).

30. W.C. Tripp and H.C. Graham, "Oxidation of Si_3N_4 in the Range 1300° to 1500°C," J. Am. Ceram. Soc., 59(9-10) 399-403(1976).

31. D. Cubicciotti, K.H. Law and R.L. Jones, "The Rate Controlling Process in the Oxidation of Hot-Pressed Si_3N_4," J. Electrochem. Soc., Accelerated Brief Communications, 124, 1955-56 (1977).

32. C.M.B. Henderson and D. Taylor, "Thermal Expansion of Nitrides and Oxynitrides of Silicon," Trans. Brit. Ceram. Soc., 74, 49 (1975).

TECHNICAL REPORT DISTRIBUTION

No. of Copies	To
1	Air Force Materials Laboratory Wright-Patterson Air Force Base, Dayton, Ohio 45433
1	Dr. R. Ruh, LLS
1	Mr. K.S. Masdiyasni
1	Dr. Norman Tallon
1	Dr. Henry Graham
1	Argonne National Laboratory Mr. R.N. Singh, Materials Science Division 9700 South Cass Avenue, Argonne, Illinois 60439
1	U.S. Army Air Mobility Research and Development Laboratory J. Accurio, Director, Lewis Directorate, NASA, Lewis Research Center, 21000 Brookpark Road, Cleveland, Ohio 44135
1	U.S. Army Material Command Commanding General, Washington, D.C. 20315 CDL (Mr. N. Klien)
	Army Materials and Mechanics Research Center Director, Watertown, Massachusetts 02172
2	ATTN: DRXMR-PL
1	DRXMR-PR
1	DRXMR-CT
1	DRXMR-AP
1	DRXMR-X (Dr. Wright)
1	DRXMR-EO (Dr. Katz)
2	DRXMR-EO (Mr. Gazza)
2	DRXMR-D (Dr. Priest)
1	DRXMR-EO (Dr. Messier)
2	DRXMR-P (Dr. Burke)
1	DRXMR-EO (Dr. McCauley)
1	DRXMR-E (Dr. Larson)
1	Col. W.R. Benoit
1	U.S. Army MERDEC Command Officer, Fort Belvoir, Virginia 22060 ATTN: STSFB-EP (Mr. W. McGovern)
1	Army Missile Command Commanding General, Redstone Arsenal, Alabama 35809 ATTN: Mr. P. Ormsby

1 Army Research and Development Office
Chief Research and Development, Department of the Army
ATTN: Physical and Engineering Sciences Division,
Washington, D.C. 20315

1 Commanding Officer, Army Research Office (Durham), Bx CM,
Duke Station Durham, North Carolina 27006 ATTN: Dr. J. Hurt

1 Lt. Col. James Kennedy, Chief, Materials Branch, European
Research Office U.S. Army R&D Group, (EUR). Box 15,
FPO New York 09510

3 U.S. Army Tank-Automotive Command
Commanding General, Warren, Michigan 48090, ATTN:
AMSTA-BSL, Research Library Br, ATTN: Mr. Machala,
ATTN: Mr. Hampiriach, ATTN: Dr. Bryzik

1 Bureau of Mines
Mr. M.A. Schwartz, Tuscaloosa Metallurgy Research
Laboratory, P.O. Box 1, University, Alabama 35486

Defense Advanced Research Projects Agency, 1400 Wilson
Boulevard, Arlington, Virginia 22209

1 ATTN: Director

1 Deputy Director

1 Director of Materials Sciences - Dr. A.L. Bement

1 Deputy Director Materials Sciences -
Dr. E.C. van Reuth

1 Technical Information Office - Mr. F.A. Koether

2 Defense Documentation Center

Commander, Cameron Station, Building 5 5010 Duke Street
Alexandria, Virginia 22314

4 Department of Energy
Division of Transportation, 20 Massachusetts Avenue, N.W.
Washington, D.C. 20545
ATTN: Mr. George Thur (TEC)
Mr. Robert Shulz (TEC) Mr. John Neal (CLNRT)
Mr. Steve Wander, Division of Fossile Fuels,
Washington, D.C. 20545

1 Department of Transportation
Mr. Michael Lauriente, 400 Seventh Street, S.W.,
Washington, D.C. 20590

12 National Technical Information Service (NTIS)
U.S. Department of Commerce
2585 Port Royal Road
Springfield, Virginia 22161

1 Directorate for Energy
W.C. Christensen, Assistant for Resources, OASD (I & L), Room 2B341 Pentagon, Washington, D.C. 20301

1 Office of the Director of Defense
Mr. R.M. Standahar, Research and Engineering, Room 3D1085, Pentagon, Washington, D.C. 20301

1 USA Foreign Science and Technology Center
Commander, ATTN: AMXST-SD3, Mr. C. Petschke, 220 7th Street NE, Charlottesville, Virginia 22901

National Aeronautics and Space Administration

1 Dr. G.C. Deutsch, Assistant Director of Research (Materials), Code RR-1, NASA, Washington, D.C. 20546

1 Mr. James J. Gangler, Advanced Research and Technology Division, Code RRM, Room B556, Headquarters, Washington, D.C. 20546

3 NASA Lewis Research Center, 21000 Brookpark Road, Cleveland, Ohio 44135
ATTN: Dr. Hubert Probst
Dr. R.L. Ashbrook
Mr. C. Blankenship

1 National Bureau of Standards
Dr. John B. Wachtman, Jr., Division Chief, Inorganic Materials Division, Room A359, Materials Building, Washington, D.C. 20234

1 Dr. S. Wiederhorn, Physical Properties Section, Institute for Materials Research, Washington, D.C. 20234

1 National Science Foundation
Mr. R. Reynik, Director, Division of Materials Research, 1800 G. Street, N.W., Washington, D.C. 20550

1 Naval Air Systems Command
Mr. Irving Machlin, High Temperature Materials Division, Materials and Processes Branch, (NAIR-52031D), Department of the Navy, Washington, D.C. 20360

1 Mr. Charles F. Bersch, Department of the Navy, Washington, D.C. 20360

1 Office of Naval Research
Dr. A.M. Diness, Metallurgy Branch, Code 471, 800 N. Quincy Street, Arlington, Virginia 22217

1 Mr. R. Rice, Washington, D.C. 20390

1 Naval Ships Research and Development Center
Mr. George A. Wacker, Head Metal Physics Branch,
Annapolis, Maryland 21402, ATTN: Code 2812

2 Naval Weapons Center
ATTN: Dr. W. Thielbalr, Code 4061, China Lake,
California 93555
ATTN: Mr. F. Markarian

1 Dr. James I. Bryant, Office of the Chief of Research,
Development and Acquisition, ATTN: DAMA-CSS, the
Pentagon, Washington, D.C. 20310

Avco Corporation

1 Dr. T. Vasilos, Applied Technology Division, Lowell
Industrial Park, Lowell, Massachusetts 01851

1 Batelle Columbus Laboratories
Mr. Winston Duckworth and Mr. Lewis E. Hulbert
505 King Avenue, Columbus, Ohio 43201

1 Batelle Memorial Institute
Metals and Ceramics Information Center. 505 King
Avenue, Columbus, Ohio 43201

1 Caterpillar Tractor Company
Mr. A.R. Canady, Technical Center, Building F,
Peoria, Illinois 61602

1 Chrysler Corporation
Mr. Philip J. Willson, Chemical Research, Box 1118,
CIMS: 418-19-18, Detroit, Michigan 48231

1 Corning Glass Works
Mr. John C. Lanning, Manager, Erwin Plant, Advanced
Engine Components Department, Corning, New York 14830

2 AiResearch Manufacturing Company
Dr. F.B. Wallace, Program Manager, Advanced Tech-
nology, 402 South 36 Street Phoenix, Arizona 85010

Mr. Karsten Styhr, AiResearch Casting Company
2525 West 190 Street, Torrance, California 90505

1 The Carborundum Company
Dr. J.A. Coppola, Research & Development Div.
P.O. Box 1054, Niagara Falls, New York 14302

1 Cummins Engine Company, Incorporated
Mr. R. Kano Columbus, Indiana 47201

1 Deposits and Composites, Incorporated
Mr. Richard E. Engdahl, 1821 Michael Faraday Drive, Reston, Virginia 22090

1 Electric Power Research Institute
Dr. Arthur Cohn, P.O. Box 10412, 3412 Hillview Avenue, Palo Alto, California 94304

1 Ford Motor Company
Mr. A.F. McLean, Scientific Research Lab, 20,000 Rotunda Drive, Dearborn, Michigan 48121

1 General Motors Corporation
Dr. Morris Berg, AC Spark Plug Division, Flint, Michigan 48556

GTE Sylvania

1 Dr. J.T. Smith, Waltham Research Center, 40 Sylvan Road, Waltham, MA 02154

1 Dr. William H. Rhodes, GTE Laboratories, Waltham Research Center, 40 Sylvan Road, Waltham, Massachusettes 02154

1 Institut fur Werkstoff-Forshung
Dr. W. Bunk, DFVLR, 505 Porz-Wahn, Linder Hohe, Germany

1 International Harvester Company
Mr. A.R. Stetson, Chief, Process Research Laboratories, Mail Zone R-1, Solar Division of Int. Harvester Company, 2200 Pacific Highway, San Diego, California 92112

1 Dr. A. Metcalfe, Solar Division of International Harvester, 2200 Pacific Highway, P.O. Box 80966, San Diego, California 92138

1 Kawecki-Berylco Industries, Incorporated
Mr. R.J. Longenecker, P.O. Box 1462, Reading, Pennsylvania 19603

1 National Beryllia Corporation
Dr. Peter L. Fleischner, Haskell, New Jersey 07420

1 Norton Company
Mr. Richard A. Alliegro, One New Bond Street, Worcester, Massachusetts 01606

1 Dr. M.L. Torti, One New Bond Street, Worcester, Massachusetts 01606

1 PPG Industries, Incorporated
Mr. F.G. Stroke, Asst. Manager Market Development, 1 Gateway Center, Pittsburgh, Pennsylvania 15222

1 Raytheon Company
Dr. Stanley Waugh, Research Division, 28 Seyon Street, Waltham, Massachusetts 02154

1 Rockwell International Corporation
Dr. F.F. Lange, Science Center, 1049 Camino Dos Rios, Thousand Oaks, California 91360

1 SKF Industries, Incorporated
Harish Dalal, Engineering and Research Center, 1100 1st Avenue, King of Prussia, Pennsylvania 19406

1 Teledyne
Mr. Robert Beck, Department Head, Development Materials, 1330 Laskey Road, Toledo, Ohio 43601

1 Dr. Eli Benstien, Director of Engineering, 1330 Laskey Road, Toledo, Ohio 43601

1 United Aircraft Research Laboratories
Dr. Frank Galasso, East Hartford, Connecticut 06108

1 United Technologies Research Center
Dr. J.J. Brennan, East Hartford, Connecticut 06108

1 Westinghouse Research Lab
Dr. R.J. Bratton, Beulah Road, Pittsburgh, Pennsylvania 15235

1 Brown University
Professor Marc Richman, Engineering Division, Providence, Rhode Island 02912

1 Georgia Tech.
Mr. J.D. Walton, Jr., EES. Atlanta, Georgia 30332

1 Illinois Institute of Technology
Mr. Seymour Bortz, IIT Research Institute, 10 West 35th Street, Chicago, Illinois 43601

1 Lehigh University
Dr. R.M. Spriggs, Assistant to the President Bethlehem, Pennsylvania 18015

2 Massachusetts Institute of Technology
Professor D.W. Kingery, Room 13-4090, Cambridge, Massachusetts 02139

Professor R.L. Coble, Dept. of Metall. & Matls. Science, Bldg. 13, Cambridge, Massachusetts 02139

1 North Carolina State University
Professor Robert F. Davis, Department of Materials Science, Box 5427, Raleigh, North Carolina 27607

1 Northwestern University
Professor Morris E. Fine. The Technological Institute Dept. of Materials Science, Evanston, Illinois

1 University of California
Professor Earl R. Parker, Department of Materials Science and Engineering, 286 Hearst Mining Building Berkeley, California 94720

1 University of Illinois
Dean Daniel C. Drucker, Engineering College, Urbana, Illinois 61801

1 University of Michigan
Professor Edward E. Hucke, Materials and Metallurgical Engineering, Ann Arbor, Michigan 48104

1 Dr. Maurice J. Sinnott, Department of Chemical and Metallurgical Engineering, Ann Arbor, Michigan 48104

1 University of Utah
Professor I.B. Cutler, College of Engineering, Division of Materials Science and Engineering, Salt Lake City, Utah 84112

1 University of Washington
Dr. James I. Mueller, Department of Ceramic Engineering, 301 Roberts Hall, FB-10, Seattle, Washington, 98195

2 Authors

---

125 Total Copies Distributed

AD-A061 880 GENERAL ELECTRIC CORPORATE RESEARCH AND DEVELOPMENT --ETC F/G 11/2
DEVELOPMENT OF A SINTERING PROCESS FOR HIGH-PERFORMANCE SILICON--ETC(U)
JUL 78 S PROCHAZKA, C D GRESKOVICH DAAG46-77-C-0030
UNCLASSIFIED SRD-77-178 AMMRC-TR-78-32 NL

2 OF 2
ADA
061880

END
DATE
FILMED
3 -79
DDC

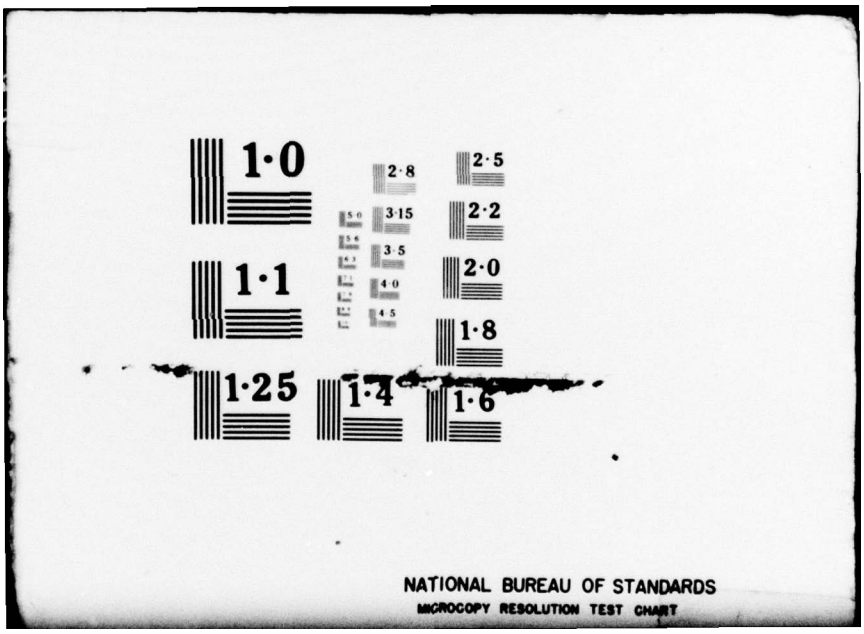
1·0
1·1
1·25
1·4
1·6
1·8
2·0
2·2
2·5
2·8
3·15
3·5
4·0
4·5
5·0
5·6
NATIONAL BUREAU OF STANDARDS
MICROCOPY RESOLUTION TEST CHART

Army Materials and Mechanics Research Center,
Watertown, Massachusetts 02172
DEVELOPMENT OF A SINTERING PROCESS
FOR HIGH-PERFORMANCE SILICON NITRIDE
S. Prochazka and C.D. Greskovich,
General Electric Company
Corporate Research and Development
Schenectady, New York 12301.

Technical Report AMMRC TR 78-32, July 1978, 77 pp-
illus - tables, Contract DAAG46-77-C-0030
Final Report, March 15, 1977 to March 15, 1978

AD _____
UNCLASSIFIED
UNLIMITED DISTRIBUTION

Key Words

Ceramic Materials
Silicon Nitride
Sintering
Nitrogen Ceramics
Beryllium Silicon Nitride
High Temperature Properties

β-Si_3N_4 ceramics with excellent creep and oxidation resistance in the temperature range of 1300 to 1450°C can be produced by the sintering process using small amounts of $BeSiN_2$ as a densification aid. Although samples have been occasionally sintered to 98% relative density, densities near 90% are routinely produced by sintering at 2000-2100°C for 15 min. in 60-80 atm of N_2. In addition to optimum amounts of Be and O required for the attainment of high density and consequently, good thermochemical properties of the ceramic, effects of metallic impurities (Ca, Mg and Fe which promote sintering)have been observed. The thermodynamic stability of Si_3N_4 is outlined and the "region of sinterability" is established for submicron α-Si_3N_4 powders containing small amounts of $BeSiN_2$.

Army Materials and Mechanics Research Center,
Watertown, Massachusetts 02172
DEVELOPMENT OF A SINTERING PROCESS
FOR HIGH-PERFORMANCE SILICON NITRIDE
S. Prochazka and C.D. Greskovich,
General Electric Company
Corporate Research and Development
Schenectady, New York 12301.

Technical Report AMMRC TR 78-32, July 1978, 77 pp-
illus - tables, Contract DAAG46-77-C-0030
Final Report, March 15, 1977 to March 15, 1978

AD _____
UNCLASSIFIED
UNLIMITED DISTRIBUTION

Key Words

Ceramic Materials
Silicon Nitride
Sintering
Nitrogen Ceramics
Beryllium Silicon Nitride
High Temperature Properties

β-Si_3N_4 ceramics with excellent creep and oxidation resistance in the temperature range of 1300 to 1450°C can be produced by the sintering process using small amounts of $BeSiN_2$ as a densification aid. Although samples have been occasionally sintered to 98% relative density, densities near 90% are routinely produced by sintering at 2000-2100°C for 15 min. in 60-80 atm of N_2. In addition to optimum amounts of Be and O required for the attainment of high density and consequently, good thermochemical properties of the ceramic, effects of metallic impurities (Ca, Mg and Fe which promote sintering)have been observed. The thermodynamic stability of Si_3N_4 is outlined and the "region of sinterability" is established for submicron α-Si_3N_4 powders containing small amounts of $BeSiN_2$.

Army Materials and Mechanics Research Center,
Watertown, Massachusetts 02172
DEVELOPMENT OF A SINTERING PROCESS
FOR HIGH-PERFORMANCE SILICON NITRIDE
S. Prochazka and C.D. Greskovich,
General Electric Company
Corporate Research and Development
Schenectady, New York 12301.

Technical Report AMMRC TR 78-32, July 1978, 77 pp-
illus - tables, Contract DAAG46-77-C-0030
Final Report, March 15, 1977 to March 15, 1978

AD _____
UNCLASSIFIED
UNLIMITED DISTRIBUTION

Key Words

Ceramic Materials
Silicon Nitride
Sintering
Nitrogen Ceramics
Beryllium Silicon Nitride
High Temperature Properties

β-Si_3N_4 ceramics with excellent creep and oxidation resistance in the temperature range of 1300 to 1450°C can be produced by the sintering process using small amounts of $BeSiN_2$ as a densification aid. Although samples have been occasionally sintered to 98% relative density, densities near 90% are routinely produced by sintering at 2000-2100°C for 15 min. in 60-80 atm of N_2. In addition to optimum amounts of Be and O required for the attainment of high density and consequently, good thermochemical properties of the ceramic, effects of metallic impurities (Ca, Mg and Fe which promote sintering)have been observed. The thermodynamic stability of Si_3N_4 is outlined and the "region of sinterability" is established for submicron α-Si_3N_4 powders containing small amounts of $BeSiN_2$.

Army Materials and Mechanics Research Center,
Watertown, Massachusetts 02172
DEVELOPMENT OF A SINTERING PROCESS
FOR HIGH-PERFORMANCE SILICON NITRIDE
S. Prochazka and C.D. Greskovich,
General Electric Company
Corporate Research and Development
Schenectady, New York 12301.

Technical Report AMMRC TR 78-32, July 1978, 77 pp-
illus - tables, Contract DAAG46-77-C-0030
Final Report, March 15, 1977 to March 15, 1978

AD _____
UNCLASSIFIED
UNLIMITED DISTRIBUTION

Key Words

Ceramic Materials
Silicon Nitride
Sintering
Nitrogen Ceramics
Beryllium Silicon Nitride
High Temperature Properties

β-Si_3N_4 ceramics with excellent creep and oxidation resistance in the temperature range of 1300 to 1450°C can be produced by the sintering process using small amounts of $BeSiN_2$ as a densification aid. Although samples have been occasionally sintered to 98% relative density, densities near 90% are routinely produced by sintering at 2000-2100°C for 15 min. in 60-80 atm of N_2. In addition to optimum amounts of Be and O required for the attainment of high density and consequently, good thermochemical properties of the ceramic, effects of metallic impurities (Ca, Mg and Fe which promote sintering)have been observed. The thermodynamic stability of Si_3N_4 is outlined and the "region of sinterability" is established for submicron α-Si_3N_4 powders containing small amounts of $BeSiN_2$.